Journal of Medicinal Chemistry

Article

Optimization of Pyrrolamide Topoisomerase II Inhibitors Towards Identification of an Antibacterial Clinical Candidate (AZD5099)

Gregory S. Basarab, Pamela J Hill, C. Edwin Garner, Kenneth Hull, Oluyinka Green, Brian A. Sherer, P. Brian Dangel, John I. Manchester, Shanta Bist, Sheila Hauck, Fei Zhou, Maria Uria-Nickelsen, Ruth Illingworth, Richard Alm, Michael Rooney, and Ann E. Eakin

J. Med. Chem., **Just Accepted Manuscript** • Publication Date (Web): 24 Jun 2014

Optimization of Pyrrolamide Topoisomerase II Inhibitors Towards Identification of an Antibacterial Clinical Candidate (AZD5099)

Gregory S. Basarab,[*] Pamela J. Hill, C. Edwin Garner,[a] Ken Hull,[b] Oluyinka Green, Brian A. Sherer,[c] P. Brian Dangel,[d] John I. Manchester, Shanta Bist, Sheila Hauck, Fei Zhou, Maria Uria-Nickelsen,[e] Ruth Illingworth, Richard Alm, Mike Rooney, and Ann E. Eakin[f]

AstraZeneca R&D Boston, Infection Innovative Medicines, 35 Gatehouse Drive, Waltham, MA 02451, USA

ABSTRACT: AZD5099 (Compound **63**) is an antibacterial agent that entered Phase 1 clinical trials targeting infections caused by Gram-positive and fastidious Gram-negative bacteria. It was derived from previously reported pyrrolamide antibacterials and a fragment based approach targeting the ATP binding site of bacterial type II topoisomerases. The program described herein varied a 3-piperidine substituent and incorporated 4-thiazole substituents that form a seven member ring intramolecular hydrogen bond with a 5-position carboxylic acid. Improved antibacterial activity and lower in vivo clearances were achieved. The lower clearances were attributed, in part, to reduced recognition by the multidrug resistant transporter Mrp2. Compound **63** showed notable efficacy in a mouse neutropenic *Staphylococcus aureus* infection model. Resistance frequency versus the drug was low, and reports of clinical resistance due to alteration of the target are few. Hence, **63** could offer a novel treatment for serious issues of resistance to currently used antibacterials.

.

INTRODUCTION

The work presented herein details optimization work in pyrrolamide antibacterial agents[1, 2] culminating in the identification of compound **63**, a drug candidate that progressed to Phase 1 human clinical trials. There is an urgent need for novel antibacterial agents effective against drug-resistant infections for which treatment options have become limited. Among the most pressing pathogens in the hospital setting are MRSA (methicillin resistant *Staphylococcus aureus*) and VRE (vancomycin resistant Enterococci). These drug-resistant Gram-positive pathogens included in a group referred to as "ESKAPE" pathogens (*Enterococcus faecium*, *S. aureus*, *Klebsiella pneumoniae*, *Acinetobacter baumannii*, *Pseudomonas aeruginosa* and *Enterobacter* spp.) that cause the majority of US hospital infections.[3-6] Pyrrolamide antibacterials (Compounds **1** and **2**, Figure 1) display potent activity against these Gram-positive pathogens and function by inhibition of the type II bacterial topoisomerases, DNA gyrase and Topoisomerase IV (Topo IV), two homologous and essential enzymes that alter DNA topology during replication.[1, 2, 7-10] DNA gyrase primarily introduces negative supercoils into DNA, while Topo IV primarily decatenates DNA during replication. Both topoisomerases exist as heterotetrameric A_2B_2 complexes, designated GyrA and GyrB for DNA gyrase, and ParC and ParE for Topo IV. The pyrrolamides are competitive with ATP, the binding site of which resides on GyrB and ParE subunits of DNA gyrase and Topo IV, respectively.[1] Extensive crystallographic studies of truncated N-terminal constructs of GyrB and ParE have been used to guide inhibitor design for the pyrrolamides and for a variety of other scaffolds that similarly bind to the ATP site of the enzymes (Figure 2).[11-16]

DNA gyrase and Topo IV are clinically validated targets for the treatment of resistant bacterial infections, with two compound classes, the fluoroquinolones[17] and aminocoumarin antibiotics,[18] inhibiting the enzymes via distinct binding sites.[19-21] The fluoroquinolones bind in the cleavage-ligation site, where they stabilize double-strand breaks in the bacterial DNA, induce rapid killing of the cells,[22] and exhibit broad-spectrum Gram-positive and Gram-negative antibacterial activity. The aminocoumarins bind the ATPase subunits of gyrase (GyrB) and, to a lesser extent, Topo IV (ParE), and exhibit Gram-positive antibacterial activity. Novobiocin (Figure 2) is the only aminocoumarin ever approved for

clinical use, but due to safety concerns and the introduction of cephalosporins, doxycycline and latter generation penicillins in the 1960s, it was not widely used and eventually withdrawn from the market.[23, 24] Widespread availability and use of the fluoroquinolones has driven the emergence of resistance to this class;[25-27] however, clinical isolates of fluoroquinolone-resistant bacteria are typically susceptible to ATPase inhibitors with no elevation of the MIC. To our knowledge, there are no well-documented examples of bacterial resistance to ATPase inhibitors in the clinic.[23, 28] The high degree of homology between GyrB and ParE, particularly in the ATP-binding region, supports the design of dual-targeting inhibitors which would minimize the development of target based bacterial resistance since the two enzymes are independently essential and independently encoded.[29] Importantly, that DNA gyrase and Topo IV are conserved across prokaryotic species offers the prospect that broad spectrum activity can be realized. Notably, DNA gyrase, only found in bacteria, is the only known prokaryotic or eukaryotic topoisomerase that traverses an energetically uphill gradient towards creating negative supercoils in DNA, rather than cleaving and re-ligating DNA single or double strands with net thermodynamically neutral energetics.[29]

A wide variety of compounds besides pyrrolamides and aminocoumarins have been shown to exhibit antibacterial activity by competing with ATP in DNA gyrase and Topo IV.[7] These include aminocoumarin mimics such as RU79115 and other natural products such as the macrocyclic cyclothialidine[30-32] and a broad range of non-natural product based heterocyclic compounds including pyrimidoindoles,[13, 33] azaindoles,[14] anilinopyridines,[34] pyrazothiazoles[16] and those with an ethylurea pharmacophore (Figure 2).[11, 12, 15, 35, 36] Although the compounds are structurally diverse, they all contain a hydrogen bond (H-bond) donating and H-bond accepting motif to an active-site aspartate and a tightly bound water, which contributes to inhibitory potencies. This H-bond donating and accepting motif mimics that seen for adenine of ATP as determined by X-ray crystallography with the 46-kDa N-terminal GyrB ATP binding domain of *E. coli*.[37] The ATP competitive inhibitors extend outside of the ATP binding pocket to a highly conserved region that participates in the dimerization of GyrB subunits following ATP binding. This dimerization involves interactions with the N-terminus from the adjacent

monomer and results in clamping of the ATPase subunits around the bacterial DNA.[38] Due to functional differences, this region is variable compared to mammalian homologues as well as to other ATPases of the GHKL protein family.[39] This is an important feature towards attaining selectivity against a myriad of ATP utilizing enzymes. The pyrrolamide compounds incorporate a pharmacophore that interacts with two arginine residues critical for dimer formation in this region of the topoisomerases.[2] Since there are significant deviations between prokaryotic and eukaryotic type II topoisomerases in this region, it was anticipated that inhibition of the latter would be minimal for analogues utilizing these binding interactions, thus reducing the risk of target-based mammalian toxicity.

The genesis of the pyrrolamide class of compounds via fragment based NMR screening against a 24-kDa N-terminal ATP binding domain of DNA gyrase from *E. coli* has been published previously.[1] A more interesting fragment, a 5-methylpyrrole carboxylic ester (Figure 1), was modeled to bind in a deep pocket of the enzyme where adenine of the ATP resides, and a program to optimize inhibitory potency against ATPase activity of DNA gyrase was initiated. A series of corresponding carboxamides was designed to extend from the pyrrole into space non-overlapping with ATP otherwise, improving inhibitory potency and leading to compound **1**. Notably, **1** demonstrated in vivo efficacy in a *S. pneumoniae* mouse lung infection model, validating the scaffold as a lead series for further optimization. A fluorine substituent on the 3-piperidine position affords two chiral centers; de-convolution of the four possible diastereomers showed highest activity in the (3*S*,4*R*)-diastereomer **2** with improved DNA gyrase inhibitory potency and antibacterial activity. A crystal structure of **2** with the N-terminal 23-kDa ATP binding domain of *Staphylococcus aureus* GyrB (PDB code 3TTZ, Figure 1) showed the pyrrole NH positioned to donate an H-bond to Asp81 and the carboxamide carbonyl positioned to accept an H-bond from a water molecule that is otherwise associated with the sidechain functionality of Asp81 and Thr173 in an H-bond array. The thiazole ring of **2** stacked against the guanidinium of Arg84 for what is considered a favorable cation-π interaction.[40] Arg84 was otherwise locked in a salt bridge with Glu58, together forming a ceiling over the inhibitor binding pocket. The thiazole carboxylic acid was positioned for a salt bridge with Arg144. The fluorine atom faced but did not closely contact a hydrophobic region of

the enzyme and may have induced a conformational bias to the piperidine ring for more favorable binding. Compound **2** also demonstrated in vivo efficacy via oral administration in a *S. pneumoniae* mouse infection model, resulting in similar reductions in measured colony forming units (CFU) at notably lower doses relative to **1**. However, species-to-species variation for the in vivo clearance (Cl) and bioavailability (F) of **2** was difficult to reconcile (see below), and an exploratory Phase 1 evaluation of the drug was carried out with oral dosing in healthy human volunteers to assess drug exposure. Ultimately, adequate drug exposure in the blood deemed necessary for reduction of bacterial burdens during an infection based on pre-clinical models could not be achieved (unpublished work). The efforts reported herein address improvement in antibacterial activity and drug exposure relative to **2** towards identification of a more efficacious drug candidate.

CHEMISTRY

Compounds were synthesized according to the general procedure shown in Scheme 1. The dichloropyrrole carboxylic acid **3** was prepared according to literature methods[41] and was coupled with aminopiperidines **4** to prepare 4-amino piperidines **5**, N-protected as a carbamate. Deprotection of the piperidine nitrogen to afford compounds **6** was followed by reaction with a substituted bromo- or chlorothiazoles **7** to afford corresponding esters of the final products. Hydrolysis of the esters led to the desired target carboxylic acids.

The 3-methoxy group on the piperidine ring imparted the best overall profile for final products (Results and Discussion), and the synthesis of the corresponding 4-amino-3-methoxypiperidine linker **4** is shown in Scheme 2, considerably shortening previous synthetic routes.[42, 43] Ethyl 4-oxopiperidine-1-carboxylate was converted to methoxypiperidine ketal **8** upon reaction with iodosobenzene diacetate and potassium hydroxide according to established procedures[44] followed by methylation with sodium hydride and methyl iodide. The intermediates for the other R3 ethers shown in Table 2 (compounds **28**- **31**) were prepared analogously as detailed in the Supporting Information. Deprotection of the ketal followed by

reductive amination with benzylamine provided **9** as a racemic mixture in a 9:1 ratio of *cis*- to *trans*-diastereomers that could be separated by chromatography to afford clean *cis* material. The benzyl group was removed via hydrogenolysis to yield the corresponding racemic 4-amino-3-methoxypiperidine **4**, which was transformed into compound **22** following the sequence of Scheme 1. Direct reductive amination with ammonium acetate in place of benzylamine to afford **4** was non-diastereoselective affording difficult to separate *cis*- and *trans*-isomers. Enantiomers of the *cis*-isomers could be obtained by chiral chromatography of **9**, but an improved separation and recovery was achieved after capping racemic **4** with the Cbz group followed by chiral chromatography to separate **10a** and **10b**, each pure to the limit of chiral HPLC analysis. The Cbz of the (+)-isomer **10b** with the (3*R*,4*S*) absolute configuration was removed *en route* to compound **23**, which proved considerably more active than the opposite enantiomer **24** derived from **10a**. The absolute configurations of **10a** and **10b** were inferred from previous work that led to compound **2**[2] in that the signs of the rotations for the analogous intermediates correlated; confirmation was achieved by a single molecule X-ray crystal structure of compound **63** (deposited in the Cambridge Crystallographic Data Center as CCDC 993908, see Supporting Information). The stereocontrolled syntheses of the other two diastereomeric 4-amino-3-methoxypiperidine linkers that were incorporated in **24** and **25** are detailed in the Supporting Information. The syntheses of piperidine linkers relevant to compounds otherwise in Table 2 are also detailed in the Supporting Material.

In the course of our investigation, a series of acyclic and cyclic ketals at the piperidine 3-position were also prepared and evaluated (Scheme 3 and Table 3). The preparation of the dimethyl ketal **39** began by conversion of ethyl 3-oxopiperidine-4-carboxylate in two steps via protection of the piperidine N-H with methylchloroformate followed by acid catalyzed ketalization with trimethylorthoformate. Hydrolysis of the ethyl ester followed by Curtius rearrangement in the presence of benzyl alcohol furnished the Cbz-protected aminopiperidine **12**. After deprotection, this was coupled to the dichloropyrrole carboxylic acid and was followed by removal of the methylcarbamate protecting group to prepare **14**. S_NAr reaction between **14** and methyl 2-bromothiazole-5-carboxylate and subsequent hydrolysis led to **39**. The sequence

to compounds **40** and **41** was carried out in an analogous fashion, and details for the synthesis of the corresponding intermediates are given in the Supporting Information. However, to synthesize a larger variety of analogs, ketal exchange from the methyl ester of **39** was more productive. To this end, the ester of **39** was heated with a given diol and an acid catalyst to produce the methyl esters of compounds **42**-**46**, which were subsequently hydrolyzed to the acids. The ketalization with 2-methoxy-1,3-propanediol produced two separable diastereomers, the esters of **42** and **43**. Extensive NMR correlations (COSY, NOESY, HMQC) failed to assign the configuration of the diastereomers, and the assignment was made only after co-crystallization of the more potent **43** with the 20.4 kDa N-terminal ParE construct of *H. influenzae* showing the methoxyl group to be positioned *syn* to the piperidine carboxamide on the ketal spirocycle (unpublished results).

A variety of carboxamides adjacent to acid of the thiazole ring were prepared via the procedure of Scheme 4. In one reaction step, thiourea and 3-chlorotetrahydrofuran-2,4-dione were cyclized in ethanol with concomitant ethanolysis to form aminothiazole **15**. TBS-protection of the alcohol followed by a Sandmeyer reaction with *tert*-butylnitrite and $CuCl_2$ yielded **16**, which was deprotected and oxidized to the chlorothiazole carboxylic acid **17** under Jones reaction conditions. Displacement of the chloride of **17** with **6a** to afford **18** enabled HATU mediated conversion to a variety of ester-amides that were hydrolyzed to the acid-amides. The amides proved to be of particular interest due to the capability of intramolecular H-bonding to the acid. The final hydrolysis step required significant optimization to avoid formation of regioisomeric acid-amides. Treatment of ester-amides with aqueous LiOH or NaOH resulted in a mixture of regioisomers often in as much as a 1:1 ratio resulting from the intermediacy of the cyclic diimide and subsequent hydrolysis. The use of $Ba(OH)_2$ in aqueous methanol enabled clean hydrolysis without cyclization to the diimide or regioisomer formation. The intermediate **16** was also used to prepare other derivatives shown in Table 4 (*i.e.* compounds **49** and **54**-**56**, **59**) via straightforward chemistry, and the synthetic details are outlined in the Supporting Information. Also analogously prepared from

commercial thiazole and benzothiazole materials were compounds **47**, **48**, **57** and **58** (Table 4) as described in the Supporting Information.

Finally, Scheme 5 summarizes the synthesis of thiazole carboxylic acids with heterocycles adjacent to the carboxylic acid towards engineering an intramolecular H-bond. A series of heterocyclic β-keto esters **19** were prepared and converted to aminothiazoles **20** by iodination and reaction with thiourea. Sandmeyer conversion to chloride or bromide and displacement with **6a** led to the desired heterocyclic thiazole esters that were converted to the acids **73**-**90**. The experimental details for the syntheses of intermediates represented by **21** are given in the Supporting Information.

RESULTS AND DISCUSSION

Enzyme inhibition (IC_{50} or the half maximal inhibitory concentration) was measured against the *S. aureus* GyrB and the *E. coli* ParE isozymes,[12] and values are listed in Tables 1-5. The rank ordering of compounds versus the two isozymes was similar, although the absolute IC_{50}s were generally 1-2 orders of magnitude lower in GyrB, wherein the IC_{50}s of more active inhibitors approached the enzyme concentration, limiting resolution below 10 nM in the routine screening assay. Thus, the ParE assay proved more robust for driving the optimization of binding affinity. A similar shift of IC_{50}s in *E. coli* ParE relative to other isozymes has been noted for other chemical series of ATPase inhibitors,[12, 33] and is partially explained by differences in residues in the hydrophobic floor that forms part of the ribose binding pocket.[45] Not all of the pyrrolamides for which IC_{50} shifts are observed interact with the hydrophobic floor, and thus this explanation is incomplete. In any case, the inhibitory potency difference between the two isozymes is not necessarily reflected in the cellular response. Both assays measure ATP hydrolysis via Malachite Green detection of phosphate release in a purified, reconstituted system which does not account for regulatory mechanisms present in the bacterial cell, or for relative expression levels of GyrB and ParE.[26] The relative importance of these enzymes for any given pathogen is best determined by genomic analysis of mutants generated to a specific inhibitor or inhibitor class.

Microbiological activity of the pyrrolamides was measured against a panel of bacterial pathogens, including two *E. coli* strains, a wild-type strain (Eco523)and a *tolC*$^{-}$ (outer membrane transport channel) strain disabled in compound efflux capability (Tables 1-5). The pyrrolamide compounds herein showed weak activity against other serious Gram-negative pathogens such as *Pseudomonas aeruginosa* and *Acinetobacter baumannii* (data not shown). Considerably lower MIC values were recorded for *E. coli tolC*$^{-}$ compared to wild-type, demonstrating that achieving effective intracellular concentrations in this, and likely other, Gram-negative organisms is problematic. Overall, the strength of the pyrrolamide class lies primarily in its Gram-positive spectrum, thereby positioning the drug class for use against skin and skin structure infections (SSSI) that are mainly caused by *S. aureus* and *Streptococcus pyogenes*. Compounds that showed activity 1 µg/mL or less versus two strains of *S. aureus*, a methicillin-sensitive strain (MSSA) and a methicillin-resistant, quinolone-resistant strain (MRQR) support the prospect of battling clinical resistance. The added activity of compounds versus *S. pneumoniae*, *Haemophilus influenzae*, *Moraxella catarrhalis* and other susceptible bacterial (data not shown) such as *Mycoplasma pneumoniae* and atypical bacterial pathogens could support treatment of community acquired bacterial pneumonia (CABP) and respiratory tract infections (RTI).

Influence of piperidine substitution and stereochemistry. The stereochemistry on the piperidine scaffold had a profound effect on activity as seen by comparing the four possible diastereomers having a C3-methoxyl substituent (compounds **23**-**26**, Table 1). The highest activity resided in the (3*S*,4*R*)-diastereomer **23**, the same configuration reported for **2**. As mentioned for **2**, the carboxamide substituent with the *R*-configuration on the piperidine ring is thought to better align the key interactions of the pyrrole NH with Asp81 and the thiazole carboxylate with Arg84 in the chiral environment of the enzyme. The methoxyl substituent in the *S*-configuration was presumed to afford better contact with a hydrophobic region below the plane of the piperidine ring from the perspective diagrammed in Figure 1, accounting for the improved potency relative to **1**. The second most active diastereomer **25** (3*R*,4*R*), epimeric at the 3-position, placed the methoxyl substituent in an allowable but unproductive environment resulting in a 2-

fold drop in *S. aureus* GyrB inhibitory potency relative to **1**. Modeling suggested that the piperidine ring of the two 4*S*-carboxamide diastereomers **24** and **26** would rotate 180° at both the 1- and 4-positions, maintaining the favorable orientations and alignments of both the pyrrole NH and the thiazole carboxylate (Figure 3). This would position the methoxyl substituent towards the inside surface of the enzyme binding pocket pushing against the well-ordered crystallographic water molecule, particularly for the 3*S*,4*S*-diastereomer. Overall, placing a methoxyl group on the piperidine C3-positon in the 4*S*-configuration led to lower biochemical potency than fluorine with the 4*S*-configuration,[2] which, in turn, was less potent than hydrogen. The ramification of these findings was that subsequent analogues focused on either racemic compounds or chiral compounds with the carboxamide in the *R*-configuration and R3 piperidine substituents oriented *cis* in the *S*-configuration. Table 2 shows the data for pyrrolamides with a variety of other substituents at the piperidine 3-position, illustrating a dilemma for the design of improved compounds. More polar compounds, as reflected in logD values, that were well accommodated for binding to GyrB and ParE might be favored in efforts to improve solubility and human plasma protein binding (PPB expressed as fraction unbound, f_u) important for clinically useful drugs. However, antibacterial activity trended lower with the increased polarity, presumably due to decreased membrane permeability. For example, incorporation of the more hydrophilic methoxyethoxyether of compound **31** at the 3-position afforded higher MIC values than the more lipophilic ethers of compounds **28**-**30**, even though inhibitory potencies were comparable. Similarly, sulfide **36** and sulfone **37** showed similar inhibitory potencies, but the greater polarity inherent in the latter led to much higher MIC values. Incorporating the chlorine atom of **35** afforded a quite potent compound, but one with exceedingly low f_u contraindicating what is deemed necessary for in vivo efficacy. Compound **38** having an azide substituent demonstrated highly potent antibacterial activity relative to **23**, which was counteracted, however, by lower f_u and higher in vivo clearance (79 mL/min/kg) in the rat. Compound **23** retained the most interesting profile taking into account antibacterial activity in combination with the other characteristics, such as PPB and clearance, important for the demonstration of efficacy *in vivo*.

Since the methoxyl group of **23** improved inhibitory potency and the epimeric methoxyl group of **25** was tolerated with only about a 2-fold decreased potency relative to **1** (see Table 1), incorporating cyclic or acyclic ketals was targeted. Modeling showed that ketals at the piperidine 3-position extend into a binding region of the enzyme where the adenine ribose of ATP resides. As the ketals were not resolved into optical antipodes, comparisons to **22**, the racemate of **23,** are made in Table 3. The MIC values for **39** with the dimethoxyketal was consistently higher than for **22** despite approximately equal enzyme inhibitory potency versus *E. coli* ParE. Activity deteriorated by formation of 5-membered ring ketal **40,** especially with regards to antibacterial activity. The 6-membered ring ketal **41** improved activity relative to the 5-membered ring ketal and **22**, albeit overall lower antibacterial activity was seen. The methoxyl-substituted 6-membered ring ketals **42** and **43** were made as a mixture of separable diastereomers, and the diastereomer **43** with the methoxyl group oriented towards the piperidine carboxamide proved more potent versus ParE than **42** with the methoxyl group oriented towards the piperidine thiazole substituent. However, the measured logD's of both compounds were lower, and MIC values were higher especially versus *S. aureus*, *H. influenza* and *M. catarrhalis*. Making spiroketal compounds more lipophilic with the dimethyl substituents of **44**, the cyclopropane of **45** and the vinyl group of **46** improved antibacterial activity. The cyclopropane ketal **45** improved inhibitory potency 20-fold relative to **22** versus ParE and displayed lower MIC values versus *H. influenzae* and *M. catarrhalis*. Despite the interesting observations with the ketals, improvements across combined considerations of antibacterial activity, PPB and clearance were not achieved. Additionally, with the increased complexity of synthesis and diastereomer resolution, the series' prospects were diminished relative to compound **22** towards identifying a drug candidate and the 3-methoxyl substituent remained optimal.

Intramolecular H-bonding with the carboxylic acid. Placement of substituents on the carbon adjacent to the thiazole carboxylate was envisioned to reduce the acidity of the carboxylate as an avenue towards reducing polarity and thereby improving bacterial membrane permeability and consequently antibacterial activity. It appeared from modeling that this thiazole 4-position carbon would be tolerant to a variety of

substituents relative to enzyme inhibitory potency. The measured pK_a of **23** was 3.6 as determined by potentiometric titration, and engineering a higher pK_a would increase the propensity to populate the neutral carboxylic acid rather than the anionic carboxylate for better permeation through bacterial phospholipid membranes. The inductive effect of electron donating substituents should increase pK_a, and indeed compound **47** with a methyl substituent had a slightly higher measured pK_a of 3.8, which, in combination with the higher lipophilicity, were presumed to contribute to the improved antibacterial activity (Table 4). However, the added methyl substituent increased PPB and led to a propensity for decarboxylation (data not shown). It was presumed that transient protonation of the weakly basic aminothiazole provides an electron sink for decarboxylation, which would be promoted by such electron donating substituents. Increasing the donating character of substituents led to greater instability; for example, the 4-methoxyl-5-carboxylate thiazole analogue of **1** could be not isolated due to facile decarboxylation. Placement of electron withdrawing groups such as CF_2H on the thiazole led to more acidic compounds (pK_a = 3.3 for **49**) and, correspondingly, lower antibacterial activity.

It was therefore hypothesized that an electron-withdrawing group that offered an opportunity for an intramolecular H-bond would maintain stability relative to decarboxylation and increase the pK_a. It was further hypothesized that rapid clearance of **2** was a key contributing factor to the low drug concentrations in the Phase 1 evaluation due to recognition by one or more organic anion transporters (OATs) or multidrug resistance proteins (MRPs) that shuttle the drug out of circulation either from the liver or the kidneys.[46, 47] Hence, thiazole 4-position substituents adjacent to the carboxylate were envisioned to block recognition by a putative anion transporter disfavoring the interaction via steric constraints, electronic alteration of the carboxylate acidity, and/or intramolecular H-bonding to appropriately positioned heteroatoms. This led to the design and synthesis of compounds **50** and **51** wherein the geometry of thiazole carboxylate allowed for a seven-member ring H-bonding array with the carbonyl substituent as shown for the carboxamide in Figure 4. Both **50** and **51** showed improved antibacterial activity relative to **23**, in particular for *S. aureus*. This was offset by a 3.5-fold lower f_u in human plasma for the two compounds relative to **23**. Note that although human plasma f_u measurements

were used routinely for assessing compounds, select compounds were assessed for f_u across mouse, rat and dog plasma (see Table 7), and rank ordering of compounds were similar, supporting the influence on in vivo clearance. Tracking the ratio MIC/f_u became a useful parameter for assessing net improvement of compound properties acknowledging that increasing f_u often leads to greater susceptibility to clearance. This strategy is consistent with recent literature that cautions against optimizing protein binding without considering other parameters that would be affected by f_u.[48-51] Protein binding variations do not necessarily alter the exposure of pharmacologically relevant free drug concentration in that a lower f_u would also lead to lower exposure due to in vivo clearance mechanisms. Modifications that lower the MIC/f_u ratio are desirable as long as they do not increase clearance. In Tables 4, 5 and 6, the calculated MIC/f_u is included for one pathogen (MRQR *S. aureus*) as a guide for analogue progression. For example, although compound **48** showed potent enzyme inhibition (especially versus ParE) and potent antibacterial activity, the high logD correlated with a decreased f_u affording a higher MIC/f_u. This, combined with high rat clearance led to diminished interest in the compound. Relative to **23**, compounds **50** and **51** showed lower MIC/f_u and lower clearance in mouse, rat and dog (rat clearance shown in Table 4). The lower clearance for these compounds could be due partially to the lower f_u, but as previously mentioned, it was also hypothesized that analogues with intramolecular H-bonds would diminish recognition of the thiazole carboxylate by hepatic or renal transporters. The pK_as of **50** and **51** were 3.29 and 4.7, respectively, the latter being higher than the 3.6 pK_a of **23** lacking a thiazole 4-position substituent. The amide of **51** would better accept a hydrogen bond than the acetyl group of **50**, accounting for the higher pK_a. The pK_a of **50** is presumed to be lower as the electron withdrawing nature of the acetyl group has a larger influence than its capacity for donation of the electron pair in the intramolecular H-bond. The NMRs of **50** and **51** in DMSO-d_6 supported the existence of an intramolecular H-bond as the acidic hydrogen peak shifted by 0.5 and 0.4 ppm**,** respectively, downfield relative to **23**. Other amide analogues besides **51** showed a considerable shift downfield in the NMR relative to **23** including a shift of 3.4-4.0 ppm for compounds **62**-**67** and **69**-**71**. The large shift for the acid proton was seen universally across the thiazole carboxamides. Moreover, at higher pH where the carboxylic acid would be expected to be ionized as

shown in Figure 4, there is evidence for an intramolecular H-bond between the amide NH and the carboxylate anion. In the NMR of the sodium salts of secondary carboxamides, there was a downfield shift of the NH resonance by a notable 4.4 ppm (compare NMR data for compounds **51**, **62**, **63** and **65** and their corresponding sodium salts in the Experimental Procedures). This H-bond is also associated with improved antibacterial activity as it presumably improved bacterial membrane permeability at physiological pH, correlating with a higher logD for the molecules. The tertiary amides of **52** and **53** are capable of receiving an H-bond from the carboxylic acid at lower pH, thereby raising the pK_a. At higher pH, the carboxylate anion H-bonding capability is removed accounting for the lower logD and higher f_u that led to less potent antibacterial activity and higher MIC/f_u values relative to secondary amides like **51**. Similarly, compounds **54**-**56** suffered from sufficiently high MIC values and MIC/f_u to diminish interest in continued profiling of biological properties.

Density Functional Theory (DFT) calculations showed that amides adjacent to carboxylic acids can form favorable intramolecular H-bonds for 5-membered ring aromatic compounds such as thiazole but not for 6-membered aromatic rings due to the geometrical considerations. This larger C-C-C exocyclic bond angles (135.8˚) for the carbonyl substituents on a thiazole ring allow for co-planarity with the resultant 7-membered ring, thereby achieving improved orbital overlap for the intramolecular H-bond. By contrast, the smaller 128.3˚ angles for such substituents on a 6-membered aromatic ring did not allow for co-planarity without significant strain. Figure 5 shows the comparison of optimized geometries for the substituents on thiazole and pyridine for both the carboxylic acid species and for the anionic carboxylate species. The side view shows graphically the distortion from co-planarity for the benzene example. Whereas the pK_a is increased in the case of the thiazole ring, the pK_a for benzoic acid decreased from 4.2 to 3.8 on incorporation of a vicinal carboxamide.[52]

The alternative thiazole substitution pattern with the carboxylate at the thiazole 4-position and substituents at the 5-positon (compounds **57**-**60**, Table 4) was also investigated. A model maintaining a salt bridge between the carboxylate of the compounds and Arg144 pointed the thiazole nitrogen atom towards the enzyme surface. A less favorable interaction is expected between the thiazole nitrogen atom

and the backbone carbonyl of the GyrB Gly83 relative to a thiazole sulfur atom due to the polarizability of the sulfur allowing for a weak non-bonding interaction as supported by analyses of the Protein Data Bank.[53, 54] Hence, **57**-**60** were less active without improving PPB or clearance. Therefore, further analogue work focused on identifying substituents on thiazole-5-carboxylic acids. To this end the series of primary carboxamides akin to **51** were evaluated targeting a relatively narrow logD range of 1-2. In line with previously mentioned observations, more polar compounds such as **70** and **72** trended to higher MIC/f_u due to higher MIC values. Compounds **67**-**69** exhibited moderately higher rat in vivo clearance relative to **51** and **62**-**66**. Compounds **62**-**66** maintained a relatively narrow logD range, higher solubilities, favorably low MIC/f_u ratios and low clearances, leading to their selection for further profiling as drug candidates.

Table 6 shows a series of 5-thiazole carboxylic acids substituted at the 4-position with heterocycles having nitrogen atoms positioned to accept an intramolecular H-bond (except **77**). The range of more basic heterocycles expands upon the quite similar H-bonding capabilities of the Table 5 carboxamides. With this, the heterocycles were envisioned to raise the pK_a of the acids leading, as suggested previously, to improved bacterial membrane permeability and antibacterial activity. That the position of the nitrogen atom is important was illustrated by pyrimidine **77**, which lacks the capability for intramolecular H-bonding and showed higher MIC values and a notably higher MIC/f_u ratio than the isomeric pyrimidines **75** and **76**. Overall, incorporation of pyrazines, pyrimidines and triazoles as in **73**-**76** offered a favorable combination of antibacterial activity, PPB, solubility and in vivo clearance. Presumably a balance is needed between the basicity of the heterocycle and the resultant physicochemical properties. The pK_as were indeed elevated for the heterocycles with values of 4.5 for triazole **74**, 5.2 and 5.7 for pyrimidines **75** and **76**, and 5.4 for pyrazine **73**. The more highly basic heterocycles such as imidazole and pyridine (compounds **81**, **82**, **84** and **88**) presumably form stronger H-bonds with the carboxylate, raising the pK_a even higher. Imidazole compounds **81** and **84** had measured pKa's of 8.0 and 7.1, respectively. However, increasing the pK_a led to poorly soluble compounds in physiologically relevant pH 7.4 buffer, which is detrimental for advancement of a drug candidate.

Towards selecting compounds for evaluation for in vivo efficacy and to enable allometric scaling to predict human PK properties, cross-species (mouse, rat and dog) PK properties were measured (Table 7). This, in combination with in vitro data (hepatocyte clearance and PPB) was used towards predicting human PK and bioavailability. The trend already described, associating improved in vivo clearance with introduction of H-bonding substituents adjacent to the carboxylate, held across the species. For example, the clearances of **63** were 4- to 40-fold lower than those of **23** in mouse, rat and dog, which represented a significant effect even accounting for the lower f_u values for **63** across the species. To address whether the lower clearances with the added substituents could be attributed at least in part to hepatic clearance, the influence of Mrp2, the major hepatobiliary transporter for non-bile organic anions,[55] was assessed. Six compounds showed significantly lower clearance in TR^- rats, which lack functional Mrp2 relative to the wild-type Wistar rats.[56, 57] By contrast, the differential in vivo clearance for moxifloxacin between Wistar and TR^- rats was minimal despite the observation that biliary excretion and efflux into the perfusate were diminished in the TR^- rats.[58] Although there is considerable variability in the triplicate experiments carried out, the clearances of compounds **1** and **23** without the additional thiazole substituent were less differentiated from the substituted thiazole compounds in the TR^- rats relative to clearances in the wild-type. Clearly, other transporters, metabolism and conjugation of the drugs contributed to overall clearance. Towards assessing more directly the influence of pyrrolamides on Mrp2 efflux, isolated membrane preparations of the isozymes from human and rat transformed into an ovarian cell line of the insect *Spodoptera frugiperda* (Sf9) were characterized for the ATPase activity.[55, 59] Figure 6 shows the dose response curve for **23** and **63** after normalizing for background ATPase activity, the two compounds being examples of activators of both human MRP2 and rat Mrp2 ATPase activity and inhibitors of the activity, respectively. MRP2 and Mrp2 are ABC-transporters, and a compound that activates ATP hydrolysis correlates with its being a substrate. Reduction of the stimulatory effect of the reference activators, sulfasalazine for human MRP2 and probenecid for rat Mrp2, indicate slowly transported compounds or those that inhibit basal ATPase activity. As a negative control, an Sf9 cell line expressing β-galactosidase showed no activation of ATPase activity for any of the compounds tested. The higher rate

of in vivo clearance for **23** is supported to the degree that it might activate rat Mrp2, while the lower clearance for **63** might therefore correlate with its inhibition of Mrp2 activity. The data for six compounds surveyed for inhibition and activation of human MRP2 and rat Mrp2 are shown in Table 9 with a rough correlation of activators being more highly cleared *in vivo* and inhibitors less highly cleared. The caveat that expression in an insect cell line may not directly relate to the situation in mammals is well understood, but the trends do correlate. Further ramifications of the data would involve drug-drug interactions as an inhibitor like **63** might slow the clearance of other drugs that are transported by MRP2 and Mrp2.

***S. aureus* neutropenic thigh infection model.** Compounds **63**, **65**, **74** and **75** were selected for evaluation of efficacy against *S. aureus* in a neutropenic mouse thigh infection model due to a combination of superior antibacterial activity, physical properties, f_u and in vivo PK. Compound **63** was efficacious against *S. aureus* (MSSA) in the model causing a dose-dependent decrease in viable counts in the thigh (Figure 7). A maximum response of about 2-log reduction, relative to the bacterial burden at the start of treatment and a 4-log reduction relative to the control was obtained at 30 mg/kg, whereas a dose of 10-15 mg/kg led to stasis. Other compounds in the series were evaluated in the same model and the data comparing efficacy at 30 mg/kg are summarized in Table 10. Compounds **63** and **74** were equally efficacious at 30 mg/kg, resulting in a 1.5 log reduction in CFU in the thigh relative to the initial pre-treatment inoculum. Typically the untreated control shows a 2.0 log (100-fold) growth in CFU between infection and the start of treatment. These compounds had an MIC of 0.03 µg/mL against MSSA and similar f_u values in mouse. Higher compound exposure, including a higher free AUC at 30 mg/kg for compound **74**, did not result in improved efficacy, indicating that the maximal response in the model may have been achieved. Compound **65** achieved stasis at the 30 mg/kg dose and showed a further drop in CFU at higher doses (data not shown). Compound **75** did not perform well in the infection model and gave variable results, despite adjustments to the dosing regimen. The lower efficacy for **75** was generally consistent with its slightly higher MIC and higher clearance, lowering the AUC and free AUC.[60]

Biological profiling of 63. Compound **63** was chosen for progression to human clinical trials and designated AZD5099.[61] Pharmacokinetic properties and bioavailability were favorable across species, positioning the compound for both parenteral and oral administration. As reported for compound **1**,[1] the *S. aureus* antibacterial activity of **63** correlated with the inhibition of DNA synthesis as determined by the attenuation of radiolabled precursor incorporation into DNA, RNA, protein and cell wall.[12, 34, 62] Thus, at a sub-lethal concentration of **63** in *S. aureus* cultures, incorporation of ^{3}H-thymidine was reduced by $10^{3.6}$-fold, considerably higher than ^{3}H-uridine incorporation ($10^{2.8}$-fold), ^{14}C-leucine incorporation (no decrease), ^{14}C-valine incorporation (no decrease), ^{14}C-acetic acid incorporation (no decrease) and ^{14}C-N-acetylglucosamine incorporation (no decrease). It follows that RNA biosynthesis (decreased ^{3}H-uridine incorporation) would be perturbed by the leading inhibition of DNA biosynthesis. Compound **63** did not exhibit cross-resistance in a variety of drug-resistant bacteria isolated from the clinic and selected to include those resistant to the fluoroquinolone levofloxacin, the β-lactam antibiotic methicillin and the glycopeptide antibiotic vancomycin in MIC_{90} determinations shown in Table 11. As yet, there has been no indication of pre-existing resistance to **63** due to genetic alteration of bacterial topoisomerases from any clinical isolates. The frequencies of spontaneous resistance to **63** in multiple isolates of *S. pneumoniae* and *S. aureus* were all less than the detection limit ($<9.6 \times 10^{-10}$) at 4 and 8 times the concentration that prevented confluent bacterial growth, with no resistant variants emerging. The frequencies of spontaneous resistance were also very low in five *Enterococcus* spp. isolates tested, with the rates being less than or equal to 3.7×10^{-9}, and resistant variants could only be isolated in three strains at the 4 times the concentration that prevented confluent bacterial growth. In the two strains of *S. pyogenes* tested, the frequencies of spontaneous resistance to **63** ranged from 1.4×10^{-7} and less than 3.4×10^{-10} at 4 and 8 times the concentration that prevented confluent bacterial growth, respectively. Resistant variants developed at twice the MIC from four *S. aureus* isolates from the AstraZeneca Research Collection were examined by extraction of the genomic DNA followed by amplification and sequencing of the type II

topoisomerase subunit genes GyrB and ParE. Increases in MICs of 8- to 16-fold were observed, whereas there was no shift in the MIC of linezolid, consistent with the target-based mode of resistance (Table 12). Sequence analysis identified that the decrease in susceptibility coincided with a mutation in the *gyrB* encoded polypeptide, suggesting that GyrB is the primary target of **63** in *S. aureus*. Two different amino acid mutations were observed: T173A in the ARC516 and ARC2381 variants and R144I in the ARC1692 and ARC2381 variants. Both mutations are expected to disrupt key interactions with the inhibitor as Thr173 was H-bonded to the water molecule otherwise H-bonded the pyrrole carboxamide and Arg144 formed a salt-bridge with the thiazole carboxylate. Both the T173A and R144I variations were seen previously for pyrrolamides[1] and have been linked to novobiocin and coumermycin A1 resistance in *S. aureus*, where the MIC values against these compounds increased 8- to 128-fold.[63] The T173A and R144I mutants had also been identified in variants resistant to the urea benzimidazole and urea pyrimidine scaffolds that target the ATPase subunits of both GyrB and ParE in *S. aureus*, suggestive of a more balanced dual targeting.[12,14] The nature of the resistant mutants to **63** has not been fully characterized since whole genome sequencing was not carried out, and what was produced in the laboratory does not necessarily correspond to what might develop in the clinic. Overall, the low frequency of spontaneous resistance in these species suggests a reduced probability of rapid development of resistance against **63** in clinical practice.

While **63** was a potent inhibitor of bacterial type II topoisomerases, a greater than 10,000-fold selectivity was measured versus the human topoisomerase IIα where the IC_{50} in a gel-based supercoiling assay was greater than 50 μM. The compound showed no signs of mutagenicity at the highest concentrations tested in an Ames mutagenicity assay,[64] an in vitro micronucleus assay using mouse lymphoma cells,[65] and an in vitro mouse lymphoma TK assay.[66] Compound **63** showed no hERG inhibition or inhibition of other ion channels at the highest concentration tested (100 μM), representing a greater than 200-fold margin to predicted free C_{max}. Compound **63** showed no inhibition at the highest concentration of 50 μM across a series of five of the most prevalent human cytochrome P450 enzymes

(Cyp1A2, Cyp2C19, Cyp2C9, Cyp2D6 and Cyp3A4) mitigating one mode of deleterious drug-drug interactions. A more thorough analysis of the preclinical in vitro and in vivo safety characteristics of **63** will be published separately.

CONCLUSIONS

Compound **63** is a novel antibacterial that entered Phase 1 clinical trials in humans via intravenous administration to target Gram-positive infections. The pyrrolamide scaffold was initiated in a fragment-based approach that identified the pyrrole pharmacophore key to binding to an active site aspartate residue. It is noteworthy that since initial disclosures of the pyrrolamides, the structure of the natural product antibiotic kibdelomycin was shown to have a dichloropyrrole carboxamide moiety akin to that in the pyrrolamides. Kibdelomycin also showed Gram-positive antibacterial activity ascribed to its inhibition of DNA gyrase and binding to its ATP binding site.[67] It is tempting to speculate that the dichloropyrrole part of the much larger kibdelomycin molecule (molecular weight = 940) binds in a similar fashion to Asp81 as seen with the pyrrolamides. The starting pyrrole discovered via fragment-based screening has been elaborated considerably before arriving at **63**. Exploration of the 3-position of the piperidine scaffold identified the methoxyl substituent that was found to be optimal in terms of intrinsic enzyme inhibitory activity, translation to antibacterial activity and maintenance of optimal physical properties. It was important to position a carboxylic acid for a salt bridge interaction with Arg84 in a region that is not associated with ATP binding to minimize off-target toxicity that might be associated with other ATP-utilizing enzymes. There is sufficient differentiation from the ATP binding region of human topoisomerases that selectivity for pyrrolamides was achieved early during the optimization program culminating in a clear selectivity for bacterial topoisomerases for **63**. Problems were encountered, however, with higher clearances for the initially reported pyrrolamides where a lone carboxylic acid substituent was placed on a thiazole ring. Reasoning that anion transporters might recognize the carboxylic acid, the compounds were designed to have an H-bond accepting moiety on the carbon adjacent to the carboxylic acid. Modeling (and NMR data) showed a clear propensity to form such an

intramolecular H-bond with the acid and H-bond accepting group attached vicinal on the thiazole ring. Importantly, in vivo clearances across species were improved in line with diminished ATPase activity of insect cell line expressed human MRP2 and rat Mrp2 and decreased in vivo clearance recorded with Mrp2 knockout TR$^-$ rats, thereby supporting the hypothesis that transporter recognition had been partially mitigated. Although only a mouse neutropenic thigh *S. aureus* infection model is disclosed herein, **63** demonstrated efficacy in a variety of animal models of infection, positioning the compound as a Gram-positive agent for treatment of hospital lung and skin infections, especially those involving drug resistant organisms such as MRSA, VRE and those that are quinolone resistant. A more extensive characterization of the pre-clinical PK-PD characteristics of the compound, the predicted PK and dose estimates and the results of the human clinical trials will be presented in a separate publication.

EXPERIMENTAL SECTION

General Considerations All of the solvents and reagents used were obtained commercially and used as such unless noted otherwise. ^{1}H NMR spectra were recorded in $CDCl_3$ or DMSO-d_6 solutions at 300 K using a Brucker Ultrashield 300 MHz instrument or a Brucker Ultrashield 400 MHz instrument. ^{13}C NMR spectra were recorded in DMSO-d_6 solutions at 300 K and 126 MHz using a Brucker DRX-500 500 MHz instrument with a QNP cryoprobe or at 101 MHz using a Brucker Ultrashield 400 MHz instrument or at 75.5 MHz using a Brucker Ultrashield 300 MHz instrument. ^{19}F NMR spectra were recorded at 282 MHz in $CDCl_3$ or DMSO-d_6 solutions at 300 K using a Brucker Ultrashield 300 MHz instrument. Chemical shifts are reported as parts per million relative to TMS (0.00) for ^{1}H and ^{13}C NMR and $CFCl_3$ for ^{19}F NMR. High-resolution mass spectra (HRMS) were obtained using a hybrid quadrupole time-of-flight mass spectrometer (microTOFq II, Bruker Daltonics) in ESI$^+$ mode. Silica gel chromatographies were performed on an ISCO Combiflash Companion Instruments using ISCO RediSep® Flash Cartridges (particle size: 35-70 microns) or Silacycle SiliaSep® Flash Cartridges (particle size: 40-63 microns). Preparative reverse phase HPLC was carried out using YMC Pack ODS-AQ (100 × 20 mm ID, S-5 μ particle size, 12 nm pore size) on Agilent instruments. All compounds tested

possessed a purity of ≥ 95%. When not indicated, compound intermediates and reagents were purchased from chemical supply houses. All final compounds (Compounds **1**-**2**, **23**-**90**) were determined to be greater than 95% pure via analysis by one of two methods. First, reversed phase LC-MS was used with a Varian Polaris C18A, 2mm x 50mm, 3mm particle size column with DAD and ELSD and aUPLC HSS T3, 2.1 x 30 mm, 1.8 um column (peak retention time, RT, in minutes). An Agilent HP1100 (Wimington, DE, USA) LC system was used with gradient of 5 to 95% acetonitile in water with 0.1% formic acid over 4.5 minutes at 1 mL/min, then hold at 95% acetonitrile at 1.5 mL/min to 6 minutes. Injection volume was 2 µL and column temperature 30 °C. Detection was based on electrospray ionization (ESI) in positive and negative polarity using Waters ZQ mass spectrometer (Milford, MA, USA), diode-array UV detector from 210 to 400 nm, and evaporative light scattering detector (Sedex 75, Sedere, Alfortville Cedex, France). Second, reversed phase UPLC-MS (rentention times, RT, in minutes) was used with a Waters Acquity UPLC instrument with DAD and ELSD and a UPLC HSS T3, 2.1 x 30 mm, 1.8 um column and a gradient of 2 to 98% acetonitrile in water with 0.1% formic acid over 2.0 minutes at 1 mL/min. Injection volume was 1 µL and the column temperature was 30 °C. Detection was based on electrospray ionization (ESI) in positive and negative polarity using Waters ZQ mass spectrometer (Milford, MA, USA), diode-array UV detector from 210 to 400 nm, and evaporative light scattering detector (Sedex 75, Sedere, Alfortville Cedex, France).

Ethyl 3-hydroxy-4,4-dimethoxypiperidine-1-carboxylate (Scheme 2) A solution of ethyl 4-oxopiperidine-1-carboxylate (26.4 mL, 29.96 g, 175 mmol) in dry MeOH (75 mL) was added via syringe to a stirred solution of KOH (42 g, 752 mmol) in dry MeOH (100 mL) at 0 °C and under an atmosphere of N_2. After stirring form 30 min, iodobenzene diacetate (84.6 g, 262 mmol) was added portionwise over 90 min maintain a temperature near 0 °C. The reaction mixture was stirred overnight with warming to rt. After removal of solvent, the residue was diluted with water, which was extracted 3 times with EtOAc. The organic layers were combined, dried ($MgSO_4$), and concentrated. Chromatography on silica gel (10-

65% EtOAc gradient in hexanes) afforded 26.74 g (66%) of the title compound as a pale yellow oil. MS (ESI) m/z $(M+H)^+$: 233 for $C_{10}H_{19}NO_5$. ^{1}H NMR (300 MHz, $CDCl_3$) δ 1.22 (t, 3H), 1.69-1.86 (m, 2H), 2.20 (m, 2H), 2.86 (t, 1H), 3.22 (s, 3H), 3.23 (s, 3H), 3.74 (m, 1H), 3.95 (m, 2H), 4.11 (q, 2H).

Ethyl 3,4,4-trimethoxypiperidine-1-carboxylate (**8**, Scheme 2) A solution of the preceding compound (52 g, 223 mmol) in 125 mL THF was added over 30 min to a stirred solution of NaH (6.96 g, 290 mmol) in 100 mL dry THF at 0 °C and under an atmosphere of N_2. The resulting solution was stirred at 0 °C under for 15 min before adding iodomethane (18.0 mL, 290 mmol) via syringe over 5 minutes. The reaction was stirred overnight, gradually warming to rt. The reaction mixture was quenched with a small volume of water and then concentrated under vacuum. The residue was diluted with water, which was extracted with 3 times with EtOAc. The organic layers were combined, dried ($MgSO_4$), and concentrated. The crude material (54.9 g) was used without further purification in the subsequent reaction. MS (ESI) m/z $(M+H)^+$: 247 for $C_{11}H_{21}NO_5$. ^{1}H NMR (300 MHz, $CDCl_3$) δ 1.24 (t, 3H), 1.72-1.83 (m, 2H), 2.82 (m, 2H), 2.98 (t, 1H), 3.20 (s, 3H), 3.21 (s, 3H), 3.41 (s, 3H), 4.10 (q, 2H), 4.20-4.37 (m, 2H).

Ethyl 3-methoxy-4-oxopiperidine-1-carboxylate (Scheme 2) A stirred solution of the preceding compound (54.9 g, 223 mmol) and 190 mL aq H_2SO_4 in THF (300 mL) was heated at 60 °C for 2 h. After cooling to rt THF solvent was removed. Solid $NaHCO_3$ was added to the aq solution until it became basic. The solution was saturated with NaCl and extracted with CH_2Cl_2 3 times. The organic layers were combined, dried ($MgSO_4$) and concentrated to afford 44.6 g of the title compound used without further purification in the subsequent step. MS (ESI) m/z $(M+H)^+$: 201 for $C_9H_{15}NO_4$. ^{1}H NMR (300 MHz, $CDCl_3$) δ 4.17 (q, 2H), 4.05 (m, 2H), 3.69 (m, 1H), 3.45 (s, 3H), 3.30-3.4 (m, 2H), 2.4-2.60 (m, 2H), 1.28 (t, 3H).

Ethyl (3*S*,4*R*)-*rel*-4-(benzylamino)-3-methoxypiperidine-1-carboxylate (**9**, Scheme 2) Benzylamine (0.130 mL, 1.19 mmol) was added dropwise to a solution of the preceding compound (200 mg, 0.99 mmol) in 1 mL THF maintaining a temperature between 0-10 ˚C. After 30 min stirring at 0 ˚C, sodium triacetoxyborohydride (232 mg, 1.09 mmol) was added portionwise over 5 min, and the mixture was

stirred at 5 °C for 4 h and overnight at rt. After quenching with water (1.2 mL) and stirred for 10 min at 5 °C, 5 mL of 2N aq. NaOH was added. The mixture was diluted with EtOAc and washed with water. The combined aq layers were extracted with additional EtOAc, which was washed with brine. The combined organic layers were dried ($MgSO_4$), and solvent was removed to afford the title compound (256 mg, 88 %) as an oil. MS (ESI) m/z $(M+H)^+$: 293 for $C_{16}H_{24}N_2O_3$. ^{1}H NMR (300 MHz, $CDCl_3$) δ 1.16 (t, 3H), 1.50 (m, 2H), 1.89 (s, 2H), 2.66 (m, 1H), 2.89 (dd, 2H), 3.26 (s, 3H), 3.67-3.83 (m, 3H), 3.99 (m, 3H), 7.18-7.37 (m, 5H).

Ethyl (3*R*,4*S*)-*rel*-4-amino-3-methoxypiperidine-1-carboxylic acid hydrochloride salt[43] (**4**, Scheme 2) Ammonium formate (31.50 g, 500 mmol) was added as a solid to a stirred solution of the preceding compound (36.45 g, 125 mmol) and 10% palladium on activated carbon (50% wet; approximately 4 g) in methanol (250 mL) at rt and under an atmosphere of N_2. The mixture was heated to 70 °C overnight. The reaction mixture was filtered through Celite®, and solvent was removed from the filtrate. The residue was diluted with water, which was extracted with a solution of ~3% methanol in chloroform (4 times). The combined organic layers were dried ($MgSO_4$) and concentrated to afford 24.18 g (96%) of the title compound as an off-white solid. MS (ESI) m/z $(M+H)^+$: 202 for $C_9H_{18}N_2O_3$.

Ethyl (3*R*,4*S*)-*rel*-4-{[(benzyloxy)carbonyl]amino}-3-methoxypiperidine-1-carboxylate (**10**, Scheme 2) Benzyl chloroformate (3.3 mL) was added dropwise to a cold solution of **4** (5 g, 24.9 mmol) in sat. aq. $NaHCO_3$. The mixture was stirred at rt for 14 h. The white precipitate was filtered, washed with water, dried in vacuo to give the title compound as a white solid (6.66 g, 80%). MS (ESI) m/z $(M+Na)^+$: 359 for $C_{17}H_{24}N_2O_5$; ^{1}H NMR (300 MHz, $CDCl_3$) δ 1.21 (t, 3H), 1.52-1.67 (m, 2H), 3.08 (m, 2H), 3.28 (s, 3H), 3.41 (s, 2H), 3.74-3.92 (m, 2H), 3.96 (m, 2H), 4.14 (m, 1H), 5.10 (s, 2H), 7.24 (d, 1H), 7.44 (m, 5H).

Ethyl (3*R*,4*S*)-4-{[(benzyloxy)carbonyl]amino}-3-methoxypiperidine-1-carboxylate (**10a**, Scheme 2) and **ethyl (3*S*,4*R*)-4-{[(benzyloxy)carbonyl]amino}-3-methoxypiperidine-1-carboxylate** (**10b**, Scheme 2) The preceding compound **10** (6.2 g, 18.5 mmol) was separated into its enantiomers by chiral chromatography over a Chiralcel OJ column (eluant: hexanes/MeOH/EtOH;70/15/15;0.1% diethylamine;

complete separation was achieved, see Supplementary Materials). The fractions corresponding to the first chromatographic peak **10a** (3*R*,4*S* (-)isomer) were collected and evaporated yielding the title compound as a white solid (2.62 g, 42% recovery). The fractions corresponding to the second chromatographic peak **10b** (3*S*,4*R* (+)isomer) were collected and evaporated yielding the title compound as a white solid (2.71 g, 44% recovery). MS (ESI) m/z $(M+Na)^+$: 359 for $C_{17}H_{24}N_2O_5$; NMR: 1.21 (t, 3H), 1.5-1.7 (m, 2H), 3.08 (m, 2H), 3.28 (s, 3H), 3.41 (s, 2H), 3.74-3.92 (m, 2H), 3.96 (m, 2H), 4.14 (m, 1H), 5.10 (s, 2H), 7.24 (d, 1H), 7.44 (m, 5H).

Ethyl (3*S*,4*R*)-4-amino-3-methoxypiperidine-1-carboxylate hydrochloride salt (**4b**, Scheme 2) A mixture of ethyl (3*S*,4*R*)-4-(benzylamino)-3-methoxypiperidine-1-carboxylate **10b** (3.98 g, 11.8 mmol), 50 mL 1N HCl and 600 mg 10% Pd on carbon in 100 mL MeOH was degassed and placed under an H_2 atmosphere for 3 h. The mixture was filtered through a bed of diatomaceous earth, and the filtrated was concentrated to afford 2.8 g (96%) of the title compound as an off-white solid. MS (ESI) m/z $(M+H)^+$: 202 for $C_9H_{18}N_2O_3$.

Ethyl (3*R*,4*S*)-4-amino-3-methoxypiperidine-1-carboxylate hydrochloride salt (**4a**, Scheme 2) Prepared as described for **4b** from (3*R*,4*S*)-4-(benzylamino)-3-methoxypiperidine-1-carboxylate **10a** (3.0 g, 8.85 mmol), 50 mL 1N HCl and 600 mg 10% Pd on carbon in 100 mL MeOH to afford 2.1 g (96%) of product. MS (ESI) m/z $(M+H)^+$: 202 for $C_9H_{18}N_2O_3$.

Ethyl (3*S*,4*R*)-*rel*-4-[(3,4-dichloro-5-methyl-1*H*-pyrrole-2-carbonyl)amino]-3-methoxy-piperidine-1-carboxylate (Scheme 1: **5**, R1=OMe, R3 = Et, racemic) 3,4-Dichloro-5-methyl-1H-pyrrole-2-carboxylic acid (304 mg, 1.57) was dissolved in anhydrous DMF. HATU (596 mg, 1.57 mmol), HOAt (213 mg, 1.57 mmol) and DIEA (274 µl, 1.76 mmol) were added and stirred at ambient for 15 min. Ethyl (3*R*,4*S*)-*rel*-4-amino-3-methoxypiperidine-1-carboxylic acid hydrochloride salt (317 mg,1.33 mmol) was added and the mixture was stirred at ambient temperature for 18 h. The mixture was diluted with EtOAc and washed with water, 1 N HCl, aq $NaHCO_3$, water and brine before drying over Na_2SO_4. The solution was concentrated to give the title compound as a brown solid (503 mg, 100%). MS (ESI) m/z $(M+H)^+$: 378,

380 for $C_{15}H_{21}Cl_2N_3O_4$; ^{1}H NMR (300 MHz, DMSO-d_6) δ 1.29 (t, 3H), 1.79 (m, 2H), 2.27 (s, 3H), 3.12 (m, 2H), 3.30 (s, 3H), 3.37 (m, 1H), 3.83-4.16 (m, 5H), 7.25 (d, 1H), 12.23 (s, 1H).

Ethyl (3*S*,4*R*)-4-[(3,4-dichloro-5-methyl-1*H*-pyrrole-2-carbonyl)amino]-3-methoxy-piperidine-1-carboxylate (Scheme 1: **5**, R1=OMe, chiral) NMM (43.7 mL, 354 mmol) was slowly added to a mixture of 3,4-dichloro-5-methyl-1*H*-pyrrole-2-carboxylic acid[42] (19.6 g, 101 mmol), ethyl (3*S*,4*R*)-4-amino-3-methoxypiperidine-1-carboxylate **4b** (1.2 g, 5.9 mmol) and HOBt (13.6 g, 101 mmol) in 400 mL anhydrous CH_2Cl_2. After 1 h stirring, 39.9 g (182 mmol) EDC was added, and stirring was continued overnight. The mixture was washed 3 times with water, 1 N HCl, sat. aq. $NaHCO_3$ and brine. Drying ($MgSO_4$) and removal of solvent gave a yellow solid that was triturated with EtOAc to afford 31.8 g (83%) of product as a whte solid. MS (ESI) m/z $(M+H)^+$: 378, 380 for $C_{15}H_{21}Cl_2N_3O_4$; ^{1}H NMR (300 MHz, DMSO-d_6) δ 1.29 (t, 3H), 1.79 (m, 2H), 2.27 (s, 3H), 3.12 (m, 2H), 3.30 (s, 3H), 3.37 (m, 1H), 3.83-4.16 (m, 5H), 7.25 (d, 1H), 12.23 (s, 1H).

Ethyl (3*R*,4*S*)-4-[(3,4-dichloro-5-methyl-1*H*-pyrrole-2-carbonyl)amino]-3-methoxy-piperidine-1-carboxylate (Scheme 1: **5**, R1 = OMe, chiral) Prepared as described for the preceding compound from 94 mg (0.49 mmol) of 3,4-dichloro-5-methyl-1H-pyrrole-2-carboxylic acid,[42] ethyl (3*R*,4*S*)-4-amino-3-methoxypiperidine-1-carboxylate **4a** (100 mg, 0.49 mmol), 108 mg (0.49 mmol) HATU, 67 mg (0.49) HOAt, 0.86 mL (4.9 mmol) of DIEA to afford 76 mg (41%) of product. MS (ESI) m/z $(M+H)^+$: 378, 380 for $C_{15}H_{21}Cl_2N_3O_4$; ^{1}H NMR (300 MHz, DMSO-d_6) δ 1.32 (t, 3H), 1.74 (m, 2H), 2.31 (s, 3H), 3.14 (m, 2H), 3.18-3.52 (s, 3H), 3.75-4.44 (m, 5H), 7.30 (d, 1H), 12.39 (s, 1H).

3,4-Dichloro-N-(3*S*,4*R*)-*rel*-[3-methoxypiperidin-4-yl]-5-methyl-1*H*-pyrrole-2-carboxamide (Scheme 1: racemic **6a**, R1 = OMe) ethyl (3*S*,4*R*)-*rel*-4-[(3,4-dichloro-5-methyl-1*H*-pyrrole-2-carbonyl)amino]-3-methoxy-piperidine-1-carboxylate (3.85 g, 10 mmol) was suspended in anhydrous CH_3CN. Iodotrimethylsilane (2.2 mL, 15.5 mmol) was added slowly, and the reaction was heated at reflux for 4 h. The crude reaction mixture was diluted with water and acidified with 1N HCl to pH 3. The solution was extracted with EtOAc. The aq layer was basified with 50% NaOH to pH 10. The aq layer as saturated with sodium chloride and extracted with THF, dried with $MgSO_4$ and concentrated to afford the title

compound as a tan solid (2.1 g, 69%). MS (ESI) m/z $(M+H)^+$: 306 for $C_{12}H_{17}Cl_2N_3O_2$; ^{1}H NMR (300 MHz, DMSO-d_6) δ 1.61 (d, *J*=3.77 Hz, 2H), 1.76 (dt, *J*=6.50, 3.16 Hz, 1H), 2.16-2.20 (m, 3H), 2.56 - 2.69 (m, 2H), 2.90 (d, *J*=13.19 Hz, 1H), 3.18 (dd, *J*=13.75, 3.01 Hz, 1H), 3.30 - 3.35 (m, 3H), 3.56 - 3.64 (m, 1H), 4.04 - 4.15 (m, *J*=8.10, 7.72, 7.72, 3.01 Hz, 1H), 7.14 (d, *J*=8.29 Hz, 1H).

3,4-Dichloro-N-(3*S*,4*R*)-[3-methoxypiperidin-4-yl]-5-methyl-1*H*-pyrrole-2-carboxamide hydrochloride salt (Scheme 1: chiral **6a**, R1 = OMe) N_2 was bubbled through a solution of 94.3 g (249 mmol) ethyl (3*S*,4*R*)-4-[(3,4-dichloro-5-methyl-1*H*-pyrrole-2-carbonyl)amino]-3-methoxy-piperidine-1-carboxylate in 1.8 L CH_3CN for 10 min. Iodotrimethylsilane (60 mL, 411 mmol) was added dropwise, and the mixture was heated at reflux for 90 min. After cooling to rt, aq. sat. $NaHSO_3$ was added, CH_3CN was removed under reduced pressure. The residue was dissolved in hot MeOH and the mixture was acidified with conc. HCl was added until the mixture was acidic (below pH = 7). Insoluble material was filtered, and the filtrate was concentrated to afford a yellow solid that was triturated with EtOAc to afford the title compound (61 g, 71%) as a white solid. MS (ESI) m/z $(M+H)^+$: 306; ^{1}H NMR (300 MHz, DMSO-d_6) δ 1.81 (m, 2H), 2.19 (s, 3H), 3.0-3.2 (m, 3H), 3.40 (s, 3H), 3.6 (m, 2H), 4.24 (m, 1H), 7.22 (d, 1H), 12.2 (s, 1H).

Methyl 2-[(3*S*,4*R*)-4-[(3,4-dichloro-5-methyl-1*H*-pyrrole-2-carbonyl)amino]-3-methoxy-1-piperidyl]thiazole-5-carboxylate (methyl ester of **23**) A solution of 2.75 g (8.98 mol) chiral **6a**, 1.99 g (8.98 mmol) of methyl 2-bromothiazole-5-carboxylate and 3.9 mL (22.4 mmol) of DIEA in NMP (20 mL) was heated at 150 °C for 20 min. The mixture was partitioned between water and EtOAc. The organic layer was separated and washed with water and brine before being dried ($MgSO_4$) and concentrated to afford a solid that was purified by chromatography on silica gel (0-50% gradient of EtOAc in CH_2Cl_2) to afford 2.8 g (70%) of the title compound. MS (ESI) m/z $(M+H)^+$:447 for $C_{17}H_{20}Cl_2N_4O_4S$; ^{1}H NMR (300 MHz, DMSO-d_6) δ 1.87 (m, 2H), 2.05 (m, 2H), 2.27 (s, 3H), 3.01 (m, 2H), 3.25 (s, 3H), 3.65 (m, 1H), 3.83 (s, 3H), 4.12 (m, 1H), 4.46 (m, 2H), 7.40 (d, 1H), 8.00 (s, 1H), 12.38 (s, 1H).

Methyl 5-(2-aminothiazol-4-yl)-2-[(3*S*,4*R*)-4-[(3,4-dichloro-5-methyl-1*H*-pyrrole-2-carbonyl)amino]-3-methoxy-1-piperidyl]thiazole-4-carboxylate (methyl ester of **73**) Prepared as described for the methyl ester of **23** from 100 mg (0.29 mmol) of chiral **6a**, 75 mg (0.27 mmol) of methyl 2'-amino-2-chloro-(4,4'-bithiazole)-5-carboxylate (described in Supporting Information) and 61 mL $NaHCO_3$ to afford 122 mg (77%) of the title compound.MS (ESI) m/z $(M+H)^+$: 545, 547 for $C_{20}H_{22}Cl_2N_6O_4S_2$; ^{1}H NMR (300 MHz, DMSO-d_6) δ 12.16 (s, 1H), 7.18 (s, 1H), 7.15 (s, 2H), 7.07 (s, 1H), 4.22-4.35 (m, 2H), 3.95-4.05 (m, 1H), 3.68 (s, 3H), 3.55 (m, 1H), 3.40 (m, 1H), 3.38 (s, 3H), 3.34 (m, 3H), 2.18 (s, 3H), 1.7-1.8 (m, 2H).

2-[(3*S*,4*R*)-4-[(3,4-Dichloro-5-methyl-1*H*-pyrrole-2-carbonyl)amino]-3-methoxy-1-piperidyl]-5-ethoxycarbonyl-thiazole-4-carboxylic acid (**18**, Scheme 4) A mixture of 34.5 g (101 mmol) of chiral **6a**, 23.5 g (101 mmol) of 5-ethyl 2-chloro-4,5-thiazolecarboxylate (**17**, see Supporting Information) and 53 mL (303 mmol) DIEA in 300 mL NMP was heated at 100 ˚C for 85 min. After cooling to rt, the reaction mixture was poured slowly into 1 L of aq. 1N HCl. The mixture was stirred for 30 min, and solids were collected by filtration, washed with water and dried *in vacuo* to afford 44.6 g (87%) of the title compound. MS (ESI) m/z $(M+H)^+$: 505 for $C_{19}H_{22}Cl_2N_4O_6S$; ^{1}H NMR (300 MHz, DMSO-d_6) δ 1.24 (t, 3H) 1.74 (s, 2H) 2.18 (s, 3H) 3.36 (s, 4H) 3.56 (s, 1H) 3.93 (s, 1H) 4.19 (s, 3H) 4.29 (s, 2H) 7.13 (s, 1H) 12.11 (s, 1H) 13.51 (s, 1H).

Ethyl 2-[(3*S*,4*R*)-4-[(3,4-dichloro-5-methyl-1*H*-pyrrole-2-carbonyl)amino]-3-methoxy-1-piperidyl]-4-(methylcarbamoyl)thiazole-5-carboxylate (ethyl ester of **51**) A solution of **18** 1.8 g, 3.56 mmol), methylamine (1.8 mL, 2M solution in THF), HATU (1.35 g, 3.56 mmol) and triethylamine (0.55 mL, 3.96 mmol) was stirred at rt for 30 min. The crude reaction mixture was slowly poured into water and the resulting white precipitate was filtered, washed with water and dried under vacuum to yield pure product (1.2 g, 65%). MS (ESI) m/z $(M+H)^+$: 518 for $C_{20}H_{25}Cl_2N_5O_5S$; ^{1}H NMR (300 MHz, DMSO-d_6) δ 1.21 (s, 3H) 1.74 (s, 2H) 2.18 (s, 3H) 2.69 (s, 3H) 3.17 (s, 2H) 3.36 (s, 3H) 3.55 (s, 1H) 3.98 (s, 1H) 4.14 (s, 2H) 4.27 (s, 2H) 7.13 (s, 1H) 8.33 (s, 1H) 12.17 (s, 1H).

Ethyl 2-[(3*S*,4*R*)-*rel*-4-[(3,4-dichloro-5-methyl-1*H*-pyrrole-2-carbonyl)amino]-3-methoxy-1-piperidyl]-4-(morpholine-4-carbonyl)thiazole-5-carboxylate (ethyl ester of **53**) Prepared as described for the ethyl ester of **15** from 100 mg (0.20 mmol) of **18**, 83 mg (0.22 mmol) of HATU, 31 µL (0.22 mmol) TEA, and 17 µL (0.20 mmol) morpholine to afford 67 mg (58%) of product. MS (ESI) m/z $(M+H)^+$: 574, 576 for $C_{23}H_{29}Cl_2N_5O_6S$; ^{1}H NMR (300 MHz, DMSO-d_6) δ 1.21 (t, 3H) 1.74 (s, 2H) 2.17 (s, 3H) 3.11 - 3.17 (m, 2H) 3.34 (s, 3H) 3.38 (s, 1H) 3.47 - 3.59 (m, 5H) 3.62 (s, 2H) 3.87 (s, 1H) 4.17 (q, 2H) 4.29 (s, 2H) 7.13 (d, 1H) 12.13 (s, 1H).

Ethyl 2-[(3*S*,4*R*)-4-[(3,4-dichloro-5-methyl-1*H*-pyrrole-2-carbonyl)amino]-3-methoxy-1-piperidyl]-4-[[(1*S*)-2-methoxy-1-methyl-ethyl]carbamoyl]thiazole-5-carboxylate (ethyl ester of **63**) Prepared as described for the ethyl ester of **15** from 8.5 g (17 mmol) **18**, 1.5 g (17 mmol) of (*S*)-2-methoxyl-1-methyl-ethylamine, 6.5 mg (17 mmol) HATU and 2.6 mL Et_3N to afford 9.47 g (97%) of product. MS (ESI) m/z $(M+H)^+$: 576, 578 for $C_{23}H_{31}Cl_2N_5O_6S$; ^{1}H NMR (300 MHz, DMSO-d_6) δ 1.09 (d, 3H) 1.22 (t, 3H) 1.75 (s, 2H) 2.18 (s, 3H) 3.17 (s, 2H) 3.26 (s, 3H) 3.37 (s, 3H) 3.55 (s, 1H) 4.01 (d, 1H) 4.17 (d, 2H) 4.27 (s, 2H) 7.16 (s, 1H) 8.32 (d, 1H) 12.16 (s, 1H).

Ethyl 2-[(3*S*,4*R*)-4-[(3,4-dichloro-5-methyl-1*H*-pyrrole-2-carbonyl)amino]-3-methoxy-1-piperidyl]-4-[[2-methoxy-1-(methoxymethyl)ethyl]carbamoyl]thiazole-5-carboxylate (ethyl ester of **65**) Prepared as described for the ethyl ester of **15** from **18** (6.0 mg, 12 mmol), [2-methoxy-1-(methoxymethyl)ethyl]amine (1.4 mg, 12 mmol), HATU (4.5 mg, 12 mmol) and Et_3N (1.8 mL, 13 mmol) to afford 4.5 g (62%) of product. MS (ESI) m/z $(M+H)^+$: 606 for $C_{24}H_{33}Cl_2N_5O_7S$; ^{1}H NMR (300 MHz, DMSO-d_6) δ 12.17 (s, 1H), 8.41 (d, *J*=8.10 Hz, 1H), 7.15 (d, *J*=8.29 Hz, 1H), 3.90-4.32 (m, 6H), 3.55 (m, 1H), 3.3-3.5 (m, 6H), 3.26 (d, *J*=1.32 Hz, 6H), 2.19 (s, 3H), 1.69-1.82 (m, 2H), 1.22 (t, *J*=7.06 Hz, 3H).

Ethyl 2-[(3*S*,4*R*)-4-[(3,4-dichloro-5-methyl-1*H*-pyrrole-2-carbonyl)amino]-3-methoxy-1-piperidyl]-4-pyrimidin-2-yl-thiazole-5-carboxylate (ethyl ester of **75**) A suspension of 0.08 g (0.23 mmol) of chiral **6a**, 0.057 g (0.21 mmol) ethyl 2-chloro-4-pyrimidin-2-yl-1,3-thiazole-5-carboxylate (described in Supporting Information), and solid $NaHCO_3$ (0.056 g, 0.69 mmol) in 3 mL DMF was heated in a microwave reactor for 30 min at 100 °C. The reaction mixture was added dropwise to a pH 4 citric acid

buffer precipitating a solid. The solid was filtered, washed with water and dried *in vacuo* to afford the title compound (0.057 g). MS (ESI) m/z $(M+H)^+$: 539, 541 for $C_{22}H_{24}Cl_2N_6O_4S$; ^{1}H NMR (300 MHz, DMSO-d_6) δ 0.092 (t, 3H), 1.69 (m, 2H), 2.12 (s, 3H), 3.31 (m, 5H), 3.50 (s, 1H), 3.91 (q, 2H), 4.19 (m, 2H), 7.09 (d, 1H), 7.49 (t, 1H), 8.80 (d, 1H), 12.10 (s, 1H).

Ethyl 2-[(3*S*,4*R*)-4-[(3,4-dichloro-5-methyl-1*H*-pyrrole-2-carbonyl)amino]-3-methoxy-1-piperidyl]-4-pyrazin-2-yl-thiazole-5-carboxylic acid (ethyl ester of **73**) Prepared as described for the ethyl ester of **73** from 1.14 g (3.72 mmol) of chiral **6a**, 1.05 g (3.89) of ethyl 2-chloro-4-(pyrazin-2-yl)thiazole-5-carboxylate (described in Supporting Information) and 937 mg $NaHCO_3$ (11.2 mmol) to afford 1.9 g (95%) of the title compound. MS (ESI) m/z $(M+H)^+$: 539, 541 for $C_{22}H_{24}Cl_2N_6O_4S$; ^{1}H NMR (300 MHz, DMSO-d_6) δ 1.08 (t, 3H), 1.77 (m, 2H), 2.19 (s, 3H), 3.33 (s, 3H), 3.39 (s, 3H), 3.57 (s, 1H), 4.06 (q, 2H), 4.11 (m, 2H), 7.16 (d, 1H), 8.67 (d, 2H), 8.84 (s, 1H), 12.16 (s, 1H).

Methyl 2-[(3*S*,4*R*)-4-[(3,4-dichloro-5-methyl-1*H*-pyrrole-2-carbonyl)amino]-3-methoxy-1-piperidyl]-4-(2-methyl-1,2,4-triazol-3-yl)thiazole-5-carboxate (methyl ester of **74**) Prepared as described for the ethyl ester of **73** from 1.18 g (3.87 mmol) of chiral **6a**, 1.0 g (3.87 mmol) of methyl 2-chloro-4-(1-methyl-1H-1,2,4-triazol-5-yl)thiazole-5-carboxylate (described in Supporting Information) and 1.08 mL Et_3N to afford 1.5 g (73%) of the title compound. MS (ESI) m/z528, 530 $(M+H)^+$ for $C_{20}H_{23}Cl_2N_7O_4S$; ^{1}H NMR (300 MHz, DMSO-d_6) δ 1.81 (m, 2H), 2.22 (s, 3H), 3.34 (m, 4H), 3.57 (m, 1H), 3.71 (s, 6H), 4.01 (m, 1H), 4.28 (m, 2H), 7.15 (d, 1H), 8.04 (s, 1H), 12.23 (s, 1H).

4-Ethyl 1-methyl 3-oxopiperidine-1,4-dicarboxylate A mixture of 1-benzyl-4-(ethoxycarbonyl)-3-oxopiperidinium chloride (25.38 g, 85 mmol), 4.0 g 10% palladium on activated carbon in 1:1 ethanol-water (300 mL) was hydrogenated at 45 psi of H_2 on a Parr Shaker hydrogenator for 2 d. The mixture was filtered through diatomaceous earth rinsing through with ethanol. Solvent from the filtrate was removed and the residue was taken up in water and cooled to 0 °C. A cold solution of potassium carbonate (35.2 g, 255 mmol) in water (10 mL) was added followed by the dropwise addition of methyl chloroformate (16.8 mL, 217mmol). After stirring at 0 °C for 30 minutes, the reaction was warmed to rt and stirred for 1 h. The reaction mixture was extracted with 3 times with ether, and the organic extracts were dried ($MgSO_4$)

and concentrated to afford a red oil. Kugelrohr distillation under vacuum afforded product was a colorless oil which solidified to colorless crystals after several days in the refrigerator (15 g, 77%). MS (ESI) m/z $M+H^+$: 230 for $C_{10}H_{15}NO_5$; ^1H NMR (300 MHz, $CDCl_3$) δ 1.22 (t, 3H), 2.23 (t, 2H), 3.45 (t, 2H), 3.61 (s, 4H), 4.00 (s, 2H), 4.19 (q, 2H), 11.92 (s, 1H).

4-Ethyl 1-methyl 3,3-dimethoxypiperidine-1,4-dicarboxylate A solution of 20 g (87 mmol) of the preceding intermediate, 15 mL (139 mmol) trimethylorthoformate and 500 mg *p*-TsOH in 30 mL MeOH was heated at reflux overnight. The mixture was concentrated to remove MeOH and the resultant mixture was diluted with aq Na_2CO_3 and extracted 2 times with EtOAc, which was washed with brine. Drying ($MgSO_4$) and removal of solvent gave 22.1 g (92%) of the title compound as an oil. ^1H NMR (300 MHz, $CDCl_3$) δ 1.34 (t, 3H), 1.74 (m, 1H), 1.93 (m, 1H), 3.09 (m, 1H), 3.25 (2s, 6H), 3.32-3.44 (m, 2H), 3.76 (s, 3H), 3.97 (m, 1H), 4.02-4.38 (m, 3H).

3,3-Dimethoxy-1-(methoxycarbonyl)piperidine-4-carboxylic acid (**11**) To a suspension of the preceding intermediate (22.1 g, 80 mmol) and $Ba(OH)_2$ (27.5 g, 160 mmol) in 100 mL 1:1 MeOH-water was stirred at rt for 2 d. The reaction mixture was acidified with 1N HCl to pH 3 and extracted with EtOAc (3X). Drying ($MgSO_4$) and removal of solvent gave 16.6 g (84%) of the title compound as a colorless oil. ^1H NMR (300 MHz, $CDCl_3$) δ 1.83-2.06 (m, 2H), 3.04 (m, 1H), 3.25 (s, 3H), 3.37 (s, 3H), 3.32-3.52 (m, 2H), 3.73 (s, 3H), 3.82-4.09 (m, 2H).

Methyl 4-(benzyloxycarbonylamino)-3,3-dimethoxy-piperidine-1-carboxylate (**12**) Ethyl chloroformate (6.2 mL, 65 mmol) and Et_3N (9.9 mL, 71mmol) were added sequentially to a solution of **11** (14.6 g, 59 mmol) in dry acetone (200 mL) at 0 °C. After stirring at 0 °C for 1 h, a solution of sodium azide (9.6 g, 15 mmol) in water (100 mL) was added, and the reaction mixture was stirred for 30 min at 0 °C and 2 h at rt. The mixture was diluted with water and acetone was removed. The aq solution was extracted 3X with toluene, which was dried ($MgSO_4$). Benzyl alcohol (9.1 mL, 88 mmol) was added, and the reaction was heated at reflux overnight. After cooling to rt, solvent was removed and the residue was chromatographed on silica gel (gradient elution 0-30% EtOAc in CH_2Cl_2) to afford the title compound as

a colorless oil (8.2 g, 40%). ^{1}H NMR (300 MHz, $CDCl_3$) δ 1.9 (m, 2H), 3.27 (s, 3H), 3.3 (m, 3H), 3.4-3.5 (m, 4H), 3.75 (s, 3H), 3.91 (m, 1H), 5.16 (s, 2H), 7.45 (s, 5H).

Methyl 4-amino-3,3-dimethoxypiperidine-1-carboxylate (**13**) A mixture of **12** (8.4 g, 24 mmol), 10% palladium on carbon (1 g) in 200 mL ethanol was added was evacuated and backfilled with nitrogen several times before being hydrogenated under a balloon H_2 atmosphere overnight. The reaction mixture was filtered through diatomaceous earth rinsing through with ethanol, and solvent was evaporated to obtain the title compound as an oil (3.75 g, 72%). ^{1}H NMR (300 MHz, $CDCl_3$) δ 1.33-1.58 (m, 2H), 1.53–1.75 (m, 1H), 3.09-3.22 (m, 8H), 3.64 (s, 3H), 3.67-4.00 (m, 2H).

Methyl 4-{[(3,4-dichloro-5-methyl-1H-pyrrol-2-yl)carbonyl]amino}-3,3-dimethoxypiperidine-1-carboxylate A solution of 3,4-dichloro-5-methyl-1*H*-pyrrole-2-carboxylic acid (2.9 g, 14.9 mmol), the preceding intermediate (3.25 g, 14.9 mmol), HOBt (2.0 g, 14.9 mmol) and NMM (6.4 m, 52.1 mmol) in CH_2Cl_2 (100 mL) was stirred at rt for 1 h, after which EDC (5.1 g, 26.8 mmol) was added. After stirring at rt for 12 h, the mixture was washed with saturated aq $NaHCO_3$ (2X), 1N HCl (2X), water (2X), and brine. The CH_2Cl_2 was then dried ($MgSO_4$) and concentrated to afford a yellow solid. Trituration with EtOAc yielded the title compound as a white solid (3.06 g, 52%). MS (ESI) m/zM-H$^-$: 392 for $C_{15}H_{21}Cl_2N_3O_5$; ^{1}H NMR (300 MHz, DMSO-*d*$_6$) δ 1.76 (m, 2H), 2.24 (s, 3H), 3.15 (s, 3H), 3.28 (s, 3H), 3.31 (m, 2H), 3.52 (m, 2H), 3.55 (m, 1H), 3.63 (s, 3H), 4.28 (m, 1H), 7.15 (d, 1H), 12.28 (s, 1H).

3,4-Dichloro-N-(3,3-dimethoxypiperidin-4-yl)-5-methyl-1*H*-pyrrole-2-carboxamide (**14**) $Ba(OH)_2$ (3.1 g, 18 mmol) was added to a suspension of **13** (3.55 g, 3.1 mmol) in 35 mL EtOH and 5 mL water. After heating in a microwave reactor at 100 °C for 2 h and cooling to rt, the reaction mixture was diluted with methanol, and insoluble material was filtered, rinsing through MeOH. The filtrate was concentrated, and the residue was partitioned between EtOAc and water. The EtOAc was dried ($MgSO_4$) and concentrated to afford the title compound as a solid (2.5 g, 83%). MS (ESI) m/z M-H$^-$: 336, 338 for $C_{13}H_{19}Cl_2N_3O_3$; ^{1}H NMR (300 MHz, DMSO-*d*$_6$) δ 12.15 (s, 1H), 7.04 (d, *J*=7.91 Hz, 1H), 4.2 (m, 1H), 3.3 (m 1H), 3.17 (s, 3H), 3.12 (s, 3H), 2.54-2.67 (m, 2H), 2.35-2.5 (m, 2H), 2.18 (s, 3H), 1.7 (m, 1H), 1.6 (m, 1H).

Methyl 2-[4-[(3,4-dichloro-5-methyl-1H-pyrrole-2-carbonyl)amino]-3,3-dimethoxy-1-piperidyl]thiazole-5-carboxylate (methyl ester of **39**) A mixture of preceding compound (2.55 g, 7.6 mmol), methyl 2-bromo-1,3-thiazole-5-carboxylate (1.7 g, 7.6 mmol) and DIEA (2.6 mL, 15.2 mmol) in NMP (30 mL) was heated at 100 °C for 2 h. The reaction mixture was cooled to rt and then slowly poured into 0.5 N HCl. After stirring at rt for several minutes, the resulting precipitate was filtered, washed with water, and dried *in vacuo* overnight to afford 3.52 g (97%) of the title compound. MS (ESI) m/z $(M+H)^+$: 477 for $C_{18}H_{22}Cl_2N_4O_5S$; ^{1}H NMR (300 MHz, DMSO-d_6) δ 1.94 (m, 2H), 2.27 (s, 3H), 3.22 (s, 6H), 3.64 (m, 2H), 3.75 (s, 3H), 3.93 (m, 1H), 4.38 (m, 1H), 7.25 (d, 1H), 7.90 (s, 1H), 12.22 (s, 1H).

Methyl 2-[(11R)-*rel*-11-[(3,4-dichloro-5-methyl-1*H*-pyrrole-2-carbonyl)amino]-3-methoxy-1,5-dioxa-8-azaspiro[5.5]undecan-8-yl]thiazole-5-carboxylate and **methyl 2-[(11R)-*rel*-11-[(3,4-dichloro-5-methyl-1H-pyrrole-2-carbonyl)amino]-3-methoxy-1,5-dioxa-8-azaspiro[5.5]undecan-8-yl]thiazole-5-carboxylate (1:1)** (methyl esters of **42** and **43**) A mixture of the methyl ester of **39** (150 mg, 0.31 mmol), 2-methoxypropane-1,3-diol (0.30 mL) and *p*-TsOH (0.01 g) in toluene was heated at reflux overnight. The reaction mixture was washed with sat. aq. Na_2CO_3 (2X), dried ($MgSO_4$) and concentrated. The residue was chromatographed on silica gel (gradient elution 25-100% EtOAc in CH_2Cl_2) to separate 2 materials. The first eluting compound (48 mg, 30%) corresponded to a single diastereomer. MS (ESI) m/z $(M+H)^+$: 519 for $C_{20}H_{24}Cl_2N_4O_6S$; ^{1}H NMR (300 MHz, DMSO-d_6) δ 1.69 (s, 1H), 1.89 (s, 1H), 2.15 - 2.22 (m, 3H), 3.14 - 3.26 (m, 1H), 3.27 - 3.31 (m, 4H), 3.51 (s, 1H), 3.63 - 3.78 (m, 3H), 4.06 (s, 2H), 4.24 - 4.36 (m, 1H), 4.94 (s, 1H), 7.11 (d, 1H), 7.77 (s, 1H), 12.17 (s, 1H), 12.66 (s, 1H). The second eluting compound (42 mg, 27%) corresponded to a second single diastereomer. MS (ESI) m/z $(M+H)^+$: 519 for $C_{20}H_{24}Cl_2N_4O_6S$; ^{1}H NMR (300 MHz, DMSO-d_6) δ 1.64 (s, 1H), 1.99 (s, 1H), 2.18 (s, 3H), 3.17 (d, 3H), 3.23 (s, 3H), 3.72 - 3.77 (m, 2H), 3.88 (s, 2H), 3.93 - 4.04 (m, 1H), 4.12 (d, 3H), 5.06 (s, 1H), 7.26 (d, 1H), 7.85 (s, 1H), 12.12 (s, 1H).

2-[(3*S*,4*R*)-4-[(3,4-Dichloro-5-methyl-1*H*-pyrrole-2-carbonyl)amino]-3-methoxy-1-piperidyl]thiazole-5-carboxylic acid (23) A solution of the corresponding ester of **23** (2.8 g, 6.5 mmol) and 2N lithium hydroxide solution in water (100 mL, 200 mmol) in THF (100 mL) was heated at reflux

for 1 h. THF was removed to leave an aqueous solution. The mixture was acidified with 10% HCl solution, and precipitated solids were collected, washed with water and dried *in vacuo* to afford the title compound (1.45 g, 54%) as a white solid. UPLC-MS RT = 0.94 min, (ESI) m/z $(M+H)^+$: 433, 435 for $C_{16}H_{18}Cl_2N_4O_4S$; ^{1}H NMR (300 MHz, DMSO-d_6) δ 12.58 (br. s., 1H), 12.15 (s, 1H), 7.74 (s, 1H), 7.16 (d, *J*=8.5 Hz, 1H), 4.17-4.41 (m, 2H), 3.93 (d, *J*=13.0 Hz, 1H), 3.55 (br. s., 1H), 3.36 (s, 3H), 2.19 (s, 3H), 1.66-1.85 (m, 2H); ^{13}C NMR (75 MHz, DMSO-d_6) δ 173.9, 162.6, 157.6, 147.6, 127.9, 118.6, 116.4, 109.7, 108.1, 75.4, 57.0, 47.9, 47.8, 46.7, 26.1, 10.6; HRMS $[M+H]^+$ 433.0487 (theoretical 433.0499); ee >98% by chiral SFC analysis (see Supporting Information).

2-[(3α,6α,11*S*)-*rel*-11-[[(3,4-Dichloro-5-methyl-1*H*-pyrrol-2-yl)carbonyl]amino]-3-methoxy-1,5-dioxa-8-azaspiro[5.5]undec-8-yl]- 5-thiazolecarboxylic acid (42) Prepared as described for **23** from 48 mg (0.090 mmol) of the corresponding methyl ester of **42** and 0.14 mL of 2N LiOH to afford 21 mg (46%) of the title compound. UPLC-MS RT = 0.97 min, (ESI) m/z $(M+H)^+$: 505 for $C_{19}H_{22}Cl_2N_4O_6S$; ^{1}H NMR (300 MHz, DMSO-d_6) δ 12.66 (br. s., 1H), 12.17 (s, 1H), 7.77 (s, 1H), 7.11 (d, *J*=8.3 Hz, 1H), 4.96 (d, *J*=14.7 Hz, 1H), 4.22-4.40 (m, 1H), 4.05 (dt, *J*=5.2, 9.8 Hz, 2H), 3.62-3.83 (m, 3H), 3.51 (t, *J*=11.5 Hz, 1H), 3.40 (m, 1H), 3.33 (s, 3H), 3.31 (m, 1H), 3.20 (d, *J*=14.1 Hz, 1H), 2.19 (s, 3H), 1.90 (m, 1H), 1.59-1.79 (m, 1H)); ^{13}C NMR (126 MHz, DMSO-d_6) δ 173.0, 162.6, 158.0, 147.6, 128.0, 118.6, 116.7, 109.6, 108.1, 95.1, 69.7, 63.2, 62.5, 56.4, 51.3, 47.0, 40.4, 28.0, 10.6; HRMS $[M+H]^+$ 505.0713 (theoretical 505.0710).

2-[(3α,6α,11*R*)-*rel*-11-[[(3,4-Dichloro-5-methyl-1*H*-pyrrol-2-yl)carbonyl]amino]-3-methoxy-1,5-dioxa-8-azaspiro[5.5]undec-8-yl]- 5-thiazolecarboxylic acid (43) Prepared as described for **23** from 42 mg (81 mmol) of the corresponding methyl ester of **43** and 0.21 mL of 2N LiOH to afford 13 mg (32%) of the title compound. MS (ESI) m/z $(M+H)^+$: 505 for $C_{19}H_{22}Cl_2N_4O_6S$; ^{1}H NMR (300 MHz, DMSO-d_6) δ 12.65 (br. s., 1H), 12.11 (s, 1H), 7.76 (s, 1H), 7.26 (d, *J*=7.16 Hz, 1H), 5.10 (d, *J*=13.6 Hz, 1H), 4.04-4.23 (m, 2H), 3.96 (d, *J*=13.8 Hz, 1H), 3.86 (d, *J*=12.4 Hz, 1H), 3.74 (m, 1H), 3.40-3.56 (m, 1H), 3.31 (s, 3H), 3.23 (s, 2H), 3.09-3.20 (m, 2H), 2.18 (s, 3H), 2.00 (m, 1H), 1.44-1.73 (m, 1H); HRMS $[M+H]^+$ 505.0713 (theoretical 505.0710); HRMS $[M+H]^+$ 505.0697 (theoretical 505.0710).

2-[11-[(3,4-Dichloro-5-methyl-1*H*-pyrrole-2-carbonyl)amino]-5,12-dioxa-8-azadispiro[2.2.56.23]tridecan-8-yl]thiazole-5-carboxylic acid (45) Prepared as described for **23** from 145 mg (0.28 mmol) of the corresponding methyl ester of **45** and 0.42 mL of 2N LiOH to afford 16 mg (11%) of the title compound. UPLC-MS RT = 1.05 min, (ESI) m/z $(M+H)^+$: 501, 503 for $C_{20}H_{22}Cl_2N_4O_5S$; ^{1}H NMR (300 MHz, DMSO-d_6) δ 12.17 (s, 1H), 7.77 (s, 1H), 7.29 (d, *J*=7.45 Hz, 1H), 5.2 (d, *J*=14.1 Hz, 1H), 4.39 (t, *J*=11.87 Hz, 2H), 4.06-4.31 (m, 5H), 3.85-4.05 (m, 1H), 3.75 (m, 1H), 3.50 (m, 1H), 3.04-3.23 (m, 2H), 2.19 (s, 3H), 1.98 (m, 1H), 1.75 (s, 1H), 1.67 (m, 1H), 0.54 (m, 1H), 0.36 (m, 1H); HRMS $[M+H]^+$ 501.0750 (theoretical 501.0761).

2-[(3*S*,4*R*)-4-[(3,4-Dichloro-5-methyl-1*H*-pyrrole-2-carbonyl)amino]-3-methoxy-1-piperidyl]-4-pyrazin-2-yl-thiazole-5-carboxylic acid (73) Prepared as described for **23** from 1.9 g (3.5 mmol) of the corresponding ethyl ester of **73** and 1.76 mL of 2N LiOH to afford 942 mg (53 %) of the title compound. UPLC-MS RT = 1.08 min, (ESI) m/z $(M+H)^+$: 511, 513 for $C_{20}H_{20}Cl_2N_6O_4S$; ^{1}H NMR (300 MHz, DMSO-d_6) 12.69 (br. s., 1H), 8.93 (d, *J*=1.5 Hz, 1H), 8.56 (dd, *J*=1.5, 2.6 Hz, 1H), 8.43 (d, *J*=2.6 Hz, 1H), 7.38 (d, *J*=8.1 Hz, 1H), 4.21-4.36 (m, 1H), 4.09 (dd, *J*=3.1, 13.9 Hz, 1H), 3.82 (m, 1H), 3.52 (br. s., 1H), 3.35 (s, 3H), 3.17-3.27 (m, 1H), 2.18 (s, 3H), 1.59-1.90 (m, 2H); ^{13}C NMR (126 MHz, DMSO-d_6) δ 168.0, 163.5, 157.8, 150.7, 146.9, 145.4, 143.0, 141.9, 128.8, 127.7, 118.7, 110.1, 108.0, 75.3, 56.8, 47.5, 47.4, 45.5, 26.3, 10.7; HRMS $[M+H]^+$ 511.0703 (theoretical 511.0717).

2-[(3*S*,4*R*)-4-[(3,4-Dichloro-5-methyl-1*H*-pyrrole-2-carbonyl)amino]-3-methoxy-1-piperidyl]-4-(2-methyl-1,2,4-triazol-3-yl)thiazole-5-carboxylic acid (74) Prepared as described for **23** from 1.5 g (2.8 mmol) of the corresponding methyl ester of **74** and 3.5 mL of 2N NaOH to afford 1.43 g (98%) of the title compound. UPLC-MS RT = 1.10 min, (ESI) m/z $(M+H)^+$: 514, 516 for $C_{19}H_{21}Cl_2N_7O_4S$; ^{1}H NMR (300 MHz, DMSO-d_6) δ ^{1}H NMR (300 MHz, DMSO-d_6) δ 15.46 (br. s., 1H), 12.16 (s, 1H), 8.25 (s, 1H), 7.17 (d, *J*=8.3 Hz, 1H), 4.29 (m, 2H), 4.09 (s, 3H), 4.01 (m, 1H), 3.59 (m, 1H), 3.46 (br. s., 1H), 3.40-3.42 (m, 1H), 3.39 (s, 3H), 2.19 (s, 3H), 1.79 (m, 2H); ^{13}C NMR (126 MHz, DMSO-d_6) δ 170.6, 160.8, 157.6, 148.4, 147.3, 140.5, 127.9, 119.4, 118.6, 109.7, 108.1, 75.4, 57.1, 48.1, 47.7, 46.5, 38.1, 26.1, 10.6; HRMS $[M+H]^+$ 514.0834 (theoretical 514.0826). $[\alpha]^{26}_D$ = -11.2 (c = 0.19, DMSO).

2-[(3*S*,4*R*)-4-[(3,4-Dichloro-5-methyl-1*H*-pyrrole-2-carbonyl)amino]-3-methoxy-1-piperidyl]-4-pyrimidin-2-yl-thiazole-5-carboxylic acid (75) Prepared as described for **23** from 40 mg (0.074 mmol) of the corresponding ethyl ester of **75** and 0.11 mL of 2N LiOH to afford 21 mg (56%) of the title compound. UPLC-MS RT = 0.95 min, (ESI) m/z $(M+H)^+$: 511 for $C_{20}H_{20}Cl_2N_6O_4S$; ^{1}H NMR (300 MHz, DMSO-d_6) δ 12.17 (s, 1H), 9.00 (d, *J*=5.0 Hz, 2H), 7.64 (t, *J*=5.0 Hz, 1H), 7.18 (d, *J*=8.5 Hz, 1H), 4.27 (m, 2H), 4.03 (m, 1H), 3.58 (m, 1H), 3.39 (s, 3H), 2.19 (s, 3H), 1.77 (m, 2H); ^{13}C NMR (101 MHz, DMSO-d_6) δ 170.1, 161.5, 160.1, 157.7, 157.1, 151.3, 128.0, 120.9, 119.0, 118.6, 109.6, 108.1, 75.4, 57.1, 48.2, 47.8, 46.3, 26.1, 10.6; HRMS $[M+H]^+$ 511.0704 (theoretical 511.0717); $[\alpha]^{26}_D$ = -12.5 (c = 0.12, DMSO); ee >98% by chiral SFC analysis (see Supporting Information).

2-[(3*S*,4*R*)-4-[(3,4-Dichloro-5-methyl-1*H*-pyrrole-2-carbonyl)amino]-3-methoxy-1-piperidyl]-4-[(2,2-dimethyl-1,3-dioxan-5-yl)carbamoyl]thiazole-5-carboxylic acid (68) $Ba(OH)_2$ (0.16 g, 0.92 mmol) dissolved in 0.5 mL water was added to a suspension of corresponding ethyl ester of **68** (0.19 g, 0.31 mmol) in MeOH (2 mL). After stirring for 3 h, the reaction was acidified with 1N HCl and concentrated to remove MeOH. The residue was extracted with EtOAc (3X), which was dried ($MgSO_4$) and concentrated to afford the title compound as a white solid (0.059 g, 32%). UPLC-MS RT = 1.21 min, (ESI) m/z $M+H^+$: 590, 592 for $C_{23}H_{29}Cl_2N_5O_7S$. ^{1}H NMR (300 MHz, DMSO-d_6) δ 13.55 (br. s, 1H), 12.16 (s, 1H), 7.17 (d, *J*=8.3 Hz, 1H), 4.20 (m, 1H), 4.1-4.2 (m, H), 3.76-3.9 (m, 6H), 3.56-3.66 (m, 2H), 3.50 (m, 1H), 3.36 (s, 3H), 3.34 (m, 4H), 3.1-3.25 (m, 2H), 2.18 (s, 3H), 1.65-1.8 (m, 2H), 1.38 (s, 3H), 1.32 (s,3H); ^{13}C NMR (126 MHz, DMSO-d_6) δ 166.4, 163.5, 161.4, 142.7, 133.4, 127.9, 118.7, 109.7, 108.0, 97.3, 75.3, 62.3, 62.2, 56.9, 47.8, 47.4, 45.6, 43.2, 26.1, 25.9, 21.3, 10.7; HRMS $[M+H]^+$ 590.1244 (theoretical 590.1238).

2-[(3*S*,4*R*)-4-[(3,4-Dichloro-5-methyl-1*H*-pyrrole-2-carbonyl)amino]-3-methoxy-1-piperidyl]-4-(methylcarbamoyl)thiazole-5-carboxylic acid (51) Prepared as described for **68** from the corresponding ethyl ester of **51** (33.1 g, 64 mmol) and 23.8 g (170 mmol) $Ba(OH)_2$ to afford the 17.1 g (54%) of product. UPLC-MS RT = 1.10 min, (ESI) m/z $M+H^+$: 490 for $C_{18}H_{21}Cl_2N_5O_5S$; ^{1}H NMR (300 MHz, DMSO-d_6) δ 13.08 (br. s., 1H), 12.16 (s, 1H), 7.17 (d, *J*=8.5 Hz, 1H), 4.04-4.43 (m, 2H), 3.84 (m, 1H), 3.51 (m, 1H),

3.36 (s, 3H), 3.31 (s, 1H), 3.07-3.26 (m, 2H), 2.68 (m, 2H), 2.19 (s, 3H), 1.73 m, 2H); ^{13}C NMR (101 MHz, DMSO-*d*$_6$) δ 166.6, 163.8, 162.3, 157.7, 143.2, 132.5, 127.8, 118.7, 109.8, 108.1, 75.3, 56.9, 47.8, 47.5, 45.6, 26.1, 25.5, 10.6; HRMS [M+H]$^+$ 490.0708 (theoretical 490.0713);); ee >98% by chiral SFC analysis (see Supporting Information).

2-[(3*S*,4*R*)-4-[(3,4-Dichloro-5-methyl-1*H*-pyrrole-2-carbonyl)amino]-3-methoxy-1-piperidyl]-4-[[(1*S*)-2-methoxy-1-methyl-ethyl]carbamoyl]thiazole-5-carboxylic acid (63) Prepared as described for **68** from the corresponding ethyl ester of **63** (27.25 g, 47 mmol) and 24.3 g (142 mmol) $Ba(OH)_2$ to afford 24.6 g (95%) of the title compound as a white solid. UPLC-MS RT = 1.19 min, (ESI) m/z (M+H)$^+$: 548, 550 for $C_{21}H_{27}Cl_2N_5O_6S$; ^{1}H NMR (300 MHz, DMSO-d$_6$) δ 13.19 (br. s., 1H), 12.19 (br. s., 1H), 7.18 (d, *J*=8.1 Hz, 1H), 4.06-4.30 (m, 2H), 3.77-4.05 (m, 2H), 3.50 (br. s., 1H), 3.36 (s, 3H), 3.25 (s, 3H), 3.05-3.22 (m, 2H), 2.19 (s, 3H), 1.72 (d, 2H), 1.09 (d, *J*=6.8 Hz, 3H); ^{13}C NMR (75 MHz, DMSO-*d*$_6$) δ 171.9, 167.6, 165.3, 161.2, 157.8, 157.7, 147.4, 127.8, 126.1, 118.7, 109.8, 108.1, 75.3, 56.9, 47.8, 45.8, 26.0, 25.8, 21.0, 10.6; HRMS [M+H]$^+$ 548.1112 (theoretical 548.1132); $[\alpha]^{26}_D$ = -13.7 (c = 0.12, DMSO); ee >98% by chiral SFC analysis (see Supporting Information).

2-[(3*S*,4*R*)-4-{[(3,4-Dichloro-5-methyl-1*H*-pyrrol-2-yl)carbonyl]amino}-3-methoxypiperidin-1-yl]-4-{[(2*S*)-2-methoxypropyl]carbamoyl}-1,3-thiazole-5-carboxylic acid (64) Prepared as described for **68** from the corresponding ethyl ester of **64** (130 mg, 0.225 mmol) and 115 mg (0.675 mmol) $Ba(OH)_2$ to afford 93 mg (75%) of the title compound as a white solid. MS (ESI) m/z (M+H)$^+$: 548, 550 for $C_{21}H_{27}Cl_2N_5O_6S$; ^{1}H NMR (300 MHz, DMSO-*d*$_6$) δ 13.15 (s, 1H), 12.09 (s, 1H), 7.10 (d, *J*=8.1 Hz, 1H), 4.0-4.3 (m, 2H), 3.6-4.0 (m, 2H), 3.4 (m, 1H), 3.29 (s, 3H), 3.18 (s, 3H), 3.0-3.2 (m, 2H), 2.12 (s, 3H), 1.6-1.7 (m, 2H), 1.01 (d, *J*=6.6 Hz, 3H); HRMS [M+H]$^+$ 548.1120 (theoretical 548.1132).

2-[(3*S*,4*R*)-4-[(3,4-Dichloro-5-methyl-1*H*-pyrrole-2-carbonyl)amino]-3-methoxy-1-piperidyl]-4-[[2-methoxy-1-(methoxymethyl)ethyl]carbamoyl]thiazole-5-carboxylic acid (65) From the corresponding ethyl ester of **65** (1.4 g, 2.4 mmol) and 1.25 g (7.3 mmol) $Ba(OH)_2$ to afford product as a white solid (1.1 g, 79%). UPLC-MS RT = 1.17 min, (ESI) m/z (M+H)$^+$: 578 for $C_{22}H_{29}Cl_2N_5O_7S$; ^{1}H NMR (300 MHz, DMSO-*d*$_6$) δ 16.18 (s, 1H), 12.16 (s, 1H), 8.93 (t, *J*=9 Hz, 1H), 7.17 (d, *J*=8.3 Hz, 1H), 4.21-4.41 (m,

2H), 3.56 (m, 1H), 3.53 (m, 1H), 3.46-3.51 (m, 2H), 3.41-3.46 (m, 1H), 3.38 (s, 3H), 3.27 (s, 3H), 3.24 (s, 3H), 2.19 (s, 3H), 1.77 (m, 2H); ^{13}C NMR (75 MHz, DMSO-d_6) δ 168.9, 163.2, 160.4, 157.6, 143.1, 127.9, 124.1, 118.6, 109.7, 108.1, 75.5, 70.7, 70.6, 58.2, 58.2, 57.1, 49.3, 47.7, 26.1, 10.6; HRMS $[M+H]^+$ 578.1261 (theoretical 578.1238); $[\alpha]^{26}_D$ = -6.12 (c = 0.12, DMSO).; ee>98% by chiral SFC (see Supporting Information).

ACKOWLEDGMENTS

Quality Performance Services, LLC of Newark, DE performed the PK studies comparing Wistar and TR$^-$ rats. SOLVO Biotechnology of Szeged, Hungary carried out inhibition and activation studies with Sf9 cell lines expressed with Mrp2 and MRP2. We would like to thank the following individuals from AstraZeneca for their valuable technical contributions and helpful advice: Barbara Arsenault, Natascha Bezdenejnih, Elise Gorseth, Dr. Camil Joubran, Haihong Ni, Sharon Tentarelli and Dr. Johnny Yang.

ABBREVIATIONS

ABC: ATP binding cassette; CFU: colony-forming unit; Cl: clearance; F: bioavailability; f_u: fraction unbound; GyrA: the A-subunit of DNA gyrase; GyrB: the B-subunit of DNA gyrase; MRQR: methicillin resistant, quinolone resistant *S. aureus*; Mrp2: Multidrug resistant-associated protein 2; MSSA: methicillin sensitive *S. aureus*; OAT: organic anion transporter; ParC: the C-subunit of topoisomerase IV; ParE: the E-subunit of topoisomerase IV; PPB: plasma protein binding; S_NAr: nucleophilic aromatic substitution; *tolC*: gene encoding outer membrane transport channel. NMM: N-methylmorpholine; HOBt: hydroxybenzotriazole

ASSOCIATED CONTENT

Supporting Information

Included are experimental procedures for the synthesis of analogues, chiral purity determinations, biological data, and crystallography of **63**. This material is available free of charge via the Internet at http://pubs.acs.org.

AUTHOR INFORMATION

Corresponding Author

[*] Phone: (781) 839-4689; email: greg.basarab@astrazeneca.com

Present Addresses

[a] Oso Corredor Scientific Consulting, 46 Camino Barranca, Placitas, NM 87043, USA.

[b]Natural Products LINCHPIN Laboratory, Department of Chemistry, Texas A & M University, College Station, TX 77842-3012 USA

[c]EMD Serono Research and Development Institute, 45A Middlesex Turnpike, Billerica, MA 01821, USA.

[d]Current Address: LEAP PAL Parts, 8810 Westgate Park Dr., Raleigh, NC 27617, USA

[e]Current Address: Pfizer Worldwide Research and Development, 620 Memorial Drive, Cambridge, MA 02139, USA

[f]Current address: Office of Biodefense, Research Resources & Translational Research, Division of Microbiology & Infectious Diseases, NIAID, NIH, 6610 Rockledge Dr., Bethesda, MD 20892

Notes

The authors declare the following competing financial interest(s): We are or have been employed by AstraZeneca Pharmaceuticals.

References

1. Eakin, A. E.; Green, O.; Hales, N.; Walkup, G. K.; Bist, S.; Singh, A.; Mullen, G.; Bryant, J.; Embrey, K.; Gao, N.; Breeze, A.; Timms, D.; Andrews, B.; Uria-Nickelsen, M.; Demeritt, J.; Loch, J. T.; Hull, K.; Blodgett, A.; Illingworth, R. N.; Prince, B.; Boriack-Sjodin, P. A.; Hauck, S.; MacPherson, L. J.; Ni, H.; Sherer, B. Pyrrolamide DNA gyrase inhibitors: fragment-based nuclear magnetic resonance screening to identify antibacterial agents. *Antimicrob. Agents Chemother.* **2012**, *56,* 1240-1246.

2. Sherer, B. A.; Hull, K.; Green, O.; Basarab, G.; Hauck, S.; Hill, P.; Loch, J. T.,3rd; Mullen, G.; Bist, S.; Bryant, J.; Boriack-Sjodin, A.; Read, J.; DeGrace, N.; Uria-Nickelsen, M.; Illingworth, R. N.; Eakin, A. E. Pyrrolamide DNA gyrase inhibitors: optimization of antibacterial activity and efficacy. *Bioorg. Med. Chem. Lett.* **2011**, *21,* 7416-7420.

3. Rice, L. B. Progress and challenges in implementing the research on ESKAPE pathogens. *Infection Control and Hospital Epidemiology* **2010**, *31,* S7-S10.

4. Gootz, T. D. The global problem of antibiotic resistance. *Crit. Rev. Immunol.* **2010**, *30,* 79-93.

5. Boucher, H. W.; Talbot, G. H.; Bradley, J. S.; Edwards, J. E.; Gilbert, D.; Rice, L. B.; Scheld, M.; Spellberg, B.; Bartlett, J. Bad bugs, no drugs: no ESKAPE! An update from the Infectious Diseases Society of America. *Clin. Infect. Dis.* **2009**, *48,* 1-12.

6. Peterson, L. R. Bad bugs, no drugs: no ESCAPE revisited. *Clin. Infect. Dis.* **2009**, *49,* 992-993.

7. Mayer, C.; Janin, Y. L. Non-quinolone inhibitors of bacterial type IIA topoisomerases: a feat of bioisosterism. *Chem. Rev.* **2013**, *114*, 2313-2342.

8. Skedelj, V.; Tomasic, T. M.; Peterlin, L.; Zega, A. ATP-binding site of bacterial enzymes as a target for antibacterial drug design. *J. Med. Chem.* **2011**, *54,* 915-929.

9. Bates, A. D.; Maxwell, A. The role of ATP in the reactions of type II DNA topoisomerases. *Biochem. Soc. Trans.* **2010**, *38,* 438-442.

10. East, S. P.; Silver, L. L. Multitarget ligands in antibacterial research: progress and opportunities. *Expert Opin. Drug Discov.* **2013**, *8,* 143-156.

11. Axford, L. C.; Agarwal, P. K.; Anderson, K. H.; Andrau, L. N.; Atherall, J.; Barker, S.; Bennett, J. M.; Blair, M.; Collins, I.; Czaplewski, L. G.; Davies, D. T.; Gannon, C. T.; Kumar, D.; Lancett, P.; Logan, A.; Lunniss, C. J.; Mitchell, D. R.; Offermann, D. A.; Palmer, J. T.; Palmer, N.; Pitt, G. R. W.; Pommier, S.; Price, D.; Narasinga Rao, B.; Saxena, R.; Shukla, T.; Singh, A. K.; Singh, M.; Srivastava, A.; Steele, C.; Stokes, N. R.; Thomaides-Brears, H. B.; Tyndall, E. M.; Watson, D.; Haydon, D. J. Design, synthesis and biological evaluation of α-substituted isonipecotic acid benzothiazole analogues as potent bacterial type II topoisomerase inhibitors. *Bioorg. Med. Chem. Lett.* **2013**, *23,* 6598-6603.

12. Basarab, G. S.; Manchester, J. I.; Bist, S.; Boriack-Sjodin, P. A.; Dangel, B.; Illingworth, R.; Sherer, B. A.; Sriram, S.; Uria-Nickelsen, M.; Eakin, A. E. Fragment-to-hit-to-lead discovery of a novel pyridylurea scaffold of ATP competitive dual targeting type II topoisomerase inhibiting antibacterial agents. *J. Med. Chem.* **2013**, *56*, 8712-8735.

13. Tari, L. W.; Li, X.; Trzoss, M.; Bensen, D. C.; Chen, Z.; Lam, T.; Zhang, J.; Lee, S. J.; Hough, G.; Phillipson, D.; Akers-Rodriguez, S.; Cunningham, M. L.; Kwan, B. P.; Nelson, K. J.; Castellano, A.; Locke, J. B.; Brown-Driver, V.; Murphy, T. M.; Ong, V. S.; Pillar, C. M.; Shinabarger, D. L.; Nix, J.; Lightstone, F. C.; Wong, S. E.; Nguyen, T. B.; Shaw, K. J.; Finn, J. Tricyclic GyrB/ParE (TriBE) inhibitors: A new class of broad-spectrum dual-targeting antibacterial agents. *PLoS One* **2013**, *8,* e84409.

14. Manchester, J. I.; Dussault, D. D.; Rose, J. A.; Boriack-Sjodin, P. A.; Uria-Nickelsen, M.; Ioannidis, G.; Bist, S.; Fleming, P.; Hull, K. G. Discovery of a novel azaindole class of antibacterial agents targeting the ATPase domains of DNA gyrase and topoisomerase IV. *Bioorg. Med. Chem. Lett.* **2012**, *22,* 5150-5156.

15. Charifson, P. S.; Grillot, A. L.; Grossman, T. H.; Parsons, J. D.; Badia, M.; Bellon, S.; Deininger, D. D.; Drumm, J. E.; Gross, C. H.; LeTiran, A.; Liao, Y.; Mani, N.; Nicolau, D. P.; Perola, E.; Ronkin, S.; Shannon, D.; Swenson, L. L.; Tang, Q.; Tessier, P. R.; Tian, S. K.; Trudeau, M.; Wang, T.; Wei, Y.; Zhang, H.; Stamos, D. Novel dual-targeting benzimidazole urea inhibitors of DNA gyrase and topoisomerase IV possessing potent antibacterial activity: intelligent design and evolution through the judicious use of structure-guided design and structure-activity relationships. *J. Med. Chem.* **2008**, *51,* 5243-5263.

16. Ronkin, S. M.; Badia, M.; Bellon, S.; Grillot, A.; Gross, C. H.; Grossman, T. H.; Mani, N.; Parsons, J. D.; Stamos, D.; Trudeau, M.; Wei, Y.; Charifson, P. S. Discovery of pyrazolthiazoles as novel and potent inhibitors of bacterial gyrase. *Bioorg. Med. Chem. Lett.* **2010**, *20,* 2828-2831.

17. Malik, S.; Choudhary, A.; Kumar, S.; Avasthi, G. Quinolones: a therapeutic review. *J. Pharm. Res.* **2010**, *2,* 1519-1523.

18. Byrskier, A.; Klich, M. Coumarin antibiotics: Novobiocin, coumermycin, and clorobiocin. in *Antimicrobial Agents: Antibacterials and Antifungals;* Bryskier, A., Ed.; ASM Press: Washington, D.C., 2005; pp 816-825.

19. Laponogov, I.; Sohi, M. K.; Veselkov, D. A.; Pan, X.; Sawhney, R.; Thompson, A. W.; McAuley, K. E.; Fisher, L. M.; Sanderson, M. R. Structural insight into the quinolone–DNA cleavage complex of type IIA topoisomerases. *Nat. Struct. Mol. Biol.* **2009**, *16,* 667-669.

20. Bax, B. D.; Chan, P. F.; Eggleston, D. S.; Fosberry, A.; Gentry, D. R.; Gorrec, F.; Giordano, I.; Hann, M. M.; Hennessy, A.; Hibbs, M.; Huang, J.; Jones, E.; Jones, J.; Brown, K. K.; Lewis, C. J.; May, E. W.; Saunders, M. R.; Singh, O.; Spitzfaden, C. E.; Shen, C.; Shillings, A.; Theobald, A. J.; Wohlkonig, A.; Pearson, N. D.; Gwynn, M. N. Type IIA topoisomerase inhibition by a new class of antibacterial agents *Nature* **2010**, *466,* 935-942.

21. Maxwell, A. The interaction between coumarin drugs and DNA gyrase. *Mol. Microbiol.* **1993**, *9,* 681-686.

22. Dwyer, D. J.; Kohanski, M. A.; Hayete, B.; Collins, J. J. Gyrase inhibitors induce an oxidative damage cellular death pathway in Escherichia coli. *Mol. Syst. Biol.* **2007**, *3,* 91.

23. Charlton, R. W. Recent advances in antibiotics. *S. Afr. Med. J.* **1969**, *43,* 311-316.

24. Food and Drug Administration *https://www.federalregister.gov/articles/2011/01/19/2011-1000/determination-that-albamycin-novobiocin-sodium-capsule-250-milligrams-was-withdrawn-from-sale-for* (accessed 6/5/2014).

25. Bowker, K. E.; Garvey, M. I.; Noel, A. R.; Tomaselli, S. G.; MacGowan, A. P. Comparative antibacterial effects of moxifloxacin and levofloxacin on *Streptococcus pneumoniae* strains with defined mechanisms of resistance: impact of bacterial inoculum. *Antimicrob. Agents Chemother.* **2013**, *68,* 1130-1138.

26. Tao, J.; Han, J.; Wu, H.; Hu, X.; Deng, J.; Fleming, J.; Maxwell, A.; Bi, L.; Mi, K. Mycobacterium fluoroquinolone resistance protein B, a novel small GTPase, is involved in the regulation of DNA gyrase and drug resistance. *Nucleic Acids Res.* **2013**, *41,* 2370-2381.

27. Fabrega, A.; Madurga, S.; Giralt, E.; Vila, J. Mechanism of action of and resistance to quinolones. *Microb. Biotechnol.* **2009**, *2,* 40-61.

28. Muñoz, R.; Bustamante, M.; de la Campa, A. G. Ser-127-to-Leu substitution in the DNA gyrase B subunit of *Streptococcus pneumoniae* is implicated in novobiocin resistance. *J. Bacteriol.* **1995**, *177,* 4166-4170; the authors are unclear whether they are working with a clinical or laboratory derived resistance.

29. Champoux, J. J. DNA topoisomerases: structure, function, and mechanism. *Annu. Rev. Biochem.* **2001**, *70,* 369-413.

30. Angehrn, P.; Goetschi, E.; Gmuender, H.; Hebeisen, P.; Hennig, M.; Kuhn, B.; Luebbers, T.; Reindl, P.; Ricklin, F.; Schmitt-Hoffmann, A. A new DNA gyrase inhibitor subclass of the cyclothialidine family based on a bicyclic dilactam-lactone scaffold. Synthesis and antibacterial properties. *J. Med. Chem.* **2011**, *54,* 2207-2224.

31. Saíz-Urra, L.; Cabrera Pérez, M. Á.; Helguera, A. M.; Froeyen, M. Combining molecular docking and QSAR studies for modelling the antigyrase activity of cyclothialidine derivatives. *Eur. J. Med. Chem.* **2011**, *46,* 2736-2747.

32. Goetschi, E.; Angehrn, P.; Gmuender, H.; Hebeisen, P.; Link, H.; Masciadri, R.; Nielsen, J. Cyclothialidine and its congeners: A new class of DNA gyrase inhibitors. *Pharmacol. Ther.* **1993**, *60,* 367-380.

33. Tari, L. W.; Trzoss, M.; Bensen, D. C.; Li, X.; Chen, Z.; Lam, T.; Zhang, J.; Creighton, C. J.; Cunningham, M. L.; Kwan, B.; Stidham, M.; Shaw, K. J.; Lightstone, F. C.; Wong, S. E.; Nguyen, T. B.; Nix, J.; Finn, J. Pyrrolopyrimidine inhibitors of DNA gyrase B (GyrB) and topoisomerase IV (ParE). Part I: structure guided discovery and optimization of dual targeting agents with potent, broad-spectrum enzymatic activity. *Bioorg. Med. Chem. Lett.* **2013**, *23,* 1529-1536.

34. Uria-Nickelsen, M.; Neckermann, G.; Sriram, S.; Andrews, B.; Manchester, J. I.; Carcanague, D.; Stokes, S.; Hull, K. G. Novel topoisomerase inhibitors: microbiological characterisation and in vivo efficacy of pyrimidines. *Int. J. Antimicrob. Agents* **2013**, *41,* 363-371 .

35. East, S. P.; White, C. B.; Barker, O.; Barker, S.; Bennett, J.; Brown, D.; Boyd, E. A.; Brennan, C.; Chowdhury, C.; Collins, I.; Convers-Reignier, E.; Dymock, B. W.; Fletcher, R.; Haydon, D. J.; Gardiner, M.; Hatcher, S.; Ingram, P.; Lancett, P.; Mortenson, P.; Papadopoulos, K.; Smee, C.; Thomaides-Brears,

H. B.; Tye, H.; Workman, J.; Czaplewski, L. G. DNA gyrase (GyrB)/topoisomerase IV (ParE) inhibitors: synthesis and antibacterial activity. *Bioorg. Med. Chem. Lett.* **2009**, *19,* 894-899.

36. Starr, J. T.; Sciotti, R. J.; Hanna, D. L.; Huband, M. D.; Mullins, L. M.; Cai, H.; Gage, J. W.; Lockard, M.; Rauckhorst, M. R.; Owen, R. M.; Lall, M. S.; Tomilo, M.; Chen, H.; McCurdy, S. P.; Barbachyn, M. R. 5-(2-Pyrimidinyl)-imidazo[1,2-a]pyridines are antibacterial agents targeting the ATPase domains of DNA gyrase and topoisomerase IV. *Bioorg. Med. Chem. Lett.* **2009**, *19,* 5302-5306.

37. Wigley, D. B.; Davies, G. J.; Dodson, E. J.; Maxwell, A.; Dodson, G. Crystal structure of an N-terminal fragment of the DNA gyrase B protein. *Nature* **1991**, *351,* 624-629.

38. Brino, L.; Urzhumtsev, A.; Mousli, M.; Bronner, C.; Mitschler, A.; Oudet, P.; Moras, D. Dimerization of *Escherichia coli* DNA-gyrase B provides a structural mechanism for activating the ATPase catalytic center. *J. Biol. Chem.* **2000**, *275,* 9468-9475.

39. Dutta, R.; Inouye, M. GHKL, an emergent ATPase/kinase superfamily. *Trends Biochem. Sci.* **2000**, *25,* 24-28.

40. Wang, X.; Post, J.; Hore, D. K.; Hof, F. Minimalist synthetic host with stacked guanidinium ions mimics the weakened hydration shells of protein-protein interaction interfaces. *J. Org. Chem.* **2013**, *79,* 34-40.

41. Motekaitis, R. J.; Heinert, D. H.; Martell, A. E. 3,4-Dihalopyrroles. *J. Org. Chem.* **1970**, *35,* 2504-2511.

42. Kim, B. J.; Pyun, D. K.; Jung, H. J.; Kwak, H. J.; Kim, J. H.; Kim, E. J.; Jeong, W. J.; Lee, C. H. Practical synthesis of ethyl *cis*-4-amino-3-methoxy-1-piperidine carboxylate, a key intermediate of cisapride. *Synth. Commun.* **2001**, *31,* 1081-1089.

43. van Daele, G. H. P.; De Bruyn, M. F. L.; Sommen, F. M.; Janssen, M.; van Nueten, J. M.; Schuurkes, J. A. J.; Niemegeers, C. J. E.; Leysen, J. E. Synthesis of cisapride, a gastrointestinal stimulant derived from *cis*-4-amino-3-methoxypiperidine. *Drug Dev. Res.* **1986**, *8,* 225-232.

44. Zacuto, M. J.; Cai, D. α-Hydroxylation of carbonyls using iodine. *Tetrahedron Lett.* **2005**, *46,* 447-450.

45. Bellon, S.; Parsons, J. D.; Wei, Y.; Hayakawa, K.; Swenson, L. L.; Charifson, P. S.; Lippke, J. A.; Aldape, R.; Gross, C. H. Crystal structures of *Escherichia coli* topoisomerase IV ParE subunit (24 and 43 kilodaltons): a single residue dictates differences in novobiocin potency against topoisomerase IV and DNA gyrase. *Antimicrob. Agents Chemother.* **2004**, *48,* 1856-1864.

46. You, G. (Section A: Molecular, Structural, and Cellular Biology of Drug Transporters) The role of organic ion transporters in drug disposition: an update. *Curr. Drug Metab.* 2004, *5,* 55-62.

47. Volk, C. OCTs, OATs, and OCTNs: structure and function of the polyspecific organic ion transporters of the SLC22 family. *Wiley Interdiscip. Rev.: Membr. Transp. Signaling* 2014, *3,* 1-13.

48. Gonzalez, D.; Schmidt, S.; Derendorf, H. Importance of relating efficacy measures to unbound drug concentrations for anti-infective agents. *Clin. Microbiol. Rev.* **2013**, *26,* 274-288.

49. Heuberger, J.; Schmidt, S.; Derendorf, H. When is protein binding important? *J. Pharm. Sci.* **2013**, *102,* 3458-3467.

50. Smith, D. A.; Di, L.; Kerns, E. H. The effect of plasma protein binding on in vivo efficacy: misconceptions in drug discovery. *Nat Rev Drug Discov* **2010**, *9,* 929-939.

51. Berezhkovskiy, L. M. On the influence of protein binding on pharmacological activity of drugs. *J. Pharm. Sci.* **2010**, *99,* 2153-2165.

52. Thompson, J. E.; Davidow, L. *A practical guide to contemporary pharmacy practice*; Lippencott Williams & Wilkins: Baltimore, MD, 2009; Vol. Third Edition.

53. Iwaoka, M.; Takemoto, S.; Okada, M.; Tomoda, S. Weak nonbonded S···X (X = O, N, and S) interactions in proteins. Statistical and theoretical studies. *Bull. Chem. Soc. Jpn.* **2002**, *75,* 1611-1625.

54. Gregoret, L. M.; Rader, S. D.; Fletterick, R. J.; Cohen, F. E. Hydrogen bonds involving sulfur atoms in proteins. *Proteins: Struct., Funct., Bioinf.* **1991**, *9,* 99-107.

55. Literature conventions are used with 'MRP2' for human and 'Mrp2' for rat isozymes. Bakos, É.; Evers, R.; Sinkó, E.; Váradi, A.; Borst, P.; Sarkadi, B. Interactions of the human multidrug resistance proteins MRP1 and MRP2 with organic anions. *Mol. Pharmacol.* **2000**, *57,* 760-768.

56. Kitamura, T.; Jansen, P.; Hardenbrook, C.; Kamimoto, Y.; Gatmaitan, Z.; Arias, I. M. Defective ATP-dependent bile canalicular transport of organic anions in mutant (TR^-) rats with conjugated hyperbilirubinemia. *Proc. Natl. Acad. Sci. U. S. A.* **1990**, *87,* 3557-3561.

57. Oude Elferink, R.; Groen, A. K. Genetic defects in hepatobiliary transport. *Biochim. Biophys. Acta, Mol. Basis Dis.* **2002**, *1586,* 129-145.

58. Ahmed, S.; Vo, N. T. P.; Thalhammer, T.; Thalhammer, F.; Gattringer, K.; Jäger, W. Involvement of Mrp2 (Abcc2) in biliary excretion of moxifloxacin and its metabolites in the isolated perfused rat liver. *J. Pharm. Pharmacol.* **2008**, *60,* 55-62.

59. Sarkadi, B.; Price, E. M.; Boucher, R. C.; Germann, U. A.; Scarborough, G. A. Expression of the human multidrug resistance cDNA in insect cells generates a high activity drug-stimulated membrane ATPase. *J .Biol. Chem.* **1992**, *267,* 4854-4858.

60. Zeitlinger, M. A.; Derendorf, H.; Mouton, J. W.; Cars, O.; Craig, W. A.; Andes, D.; Theuretzbacher, U. Protein binding: do we ever learn? *Antimicrob. Agents Chemoth.* **2011**, *55,* 3067-3074.

61. Basarab, G.; Dangel, B.; Fleming, P. R.; Gravestock, M. B.; Green, O.; Hauck, S. I.; Hill, P.; Hull, K. G., Mullen, G.; Ni, H.; Sherer, B.; Zhou, F.; Antibacterial piperdine derivatives; USP 8399489, 2006.

62. Hilliard, J. J.; Goldschmidt, R. M.; Licata, L.; Baum, E. Z.; Bush, K. Multiple mechanisms of action for inhibitors of histidine protein kinases from bacterial two-component systems. *Antimicrob. Agents Chemother.* **1999**, *43,* 1693-1699.

63. Fujimoto-Nakamura, M.; Ito, H.; Oyamada, Y.; Nishino, T.; Yamagishi, J. Accumulation of mutations in both gyrB and parE genes is associated with high-level resistance to novobiocin in *Staphylococcus aureus*. *Antimicrob. Agents Chemother.* **2005**, *49,* 3810-3815.

64. Mortelmans, K.; Zeiger, E. The Ames salmonella/microsome mutagenicity assay. *Mutat. Res., Fundam. Mol. Mech. Mutagen.* **2000**, 455, 29-60.

65. Kirsch-Volders, M.; Elhajouji, A.; Cundari, E.; Van Hummelen, P. The in vitro micronucleus test: a multi-endpoint assay to detect simultaneously mitotic delay, apoptosis, chromosome breakage, chromosome loss and non-disjunction. *Mutat. Res., Fundam. Mol. Mech. Mutagen.* **1997**, *392,* 19-30.

66. Lloyd, M.; Kidd, D. The mouse lymphoma assay. in Parry, J. M., Parry, E. M., Eds.; Springer New York: 2012; Vol. 817, pp 35-54.

67. Phillips, J.; Goetz, M.; Smith, S.; Zink, D.; Polishook, J.; Onishi, R.; Salowe, S.; Wiltsie, J.; Allocco, J.; Sigmund, J.; Dorso, K.; Lee, S.; Skwish, S.; de la Cruz, M.; Martín, J.; Vicente, F.; Genilloud, O.; Lu, J.; Painter, R.; Young, K.; Overbye, K.; Donald, R. K.; Singh, S. Discovery of kibdelomycin, a potent new class of bacterial Type II topoisomerase inhibitor by chemical-genetic profiling in *Staphylococcus aureus*. *Chem. Biol.* **2011**, *18,* 955-965.

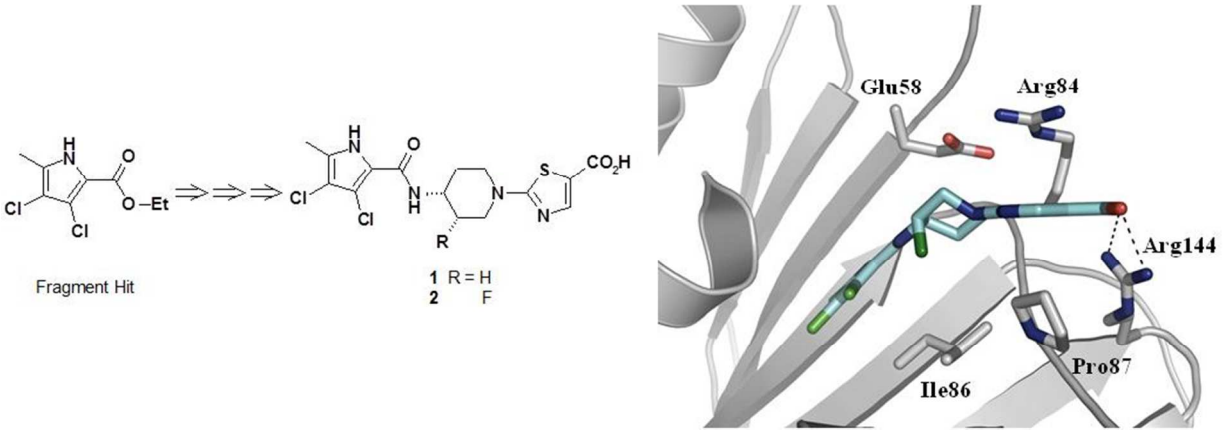

Figure 1. Structures of fragment hit and pyrrolamides **1** and **2** (left). Side-view of **2** in X-ray derived co-crystal structure complex with *S. aureus* GyrB (3TTZ) in surface stick representation (right). For clarity, key interactions of Asp81, Thr173 and the bound water associated with the pyrrole carboxamide are omitted from the view.

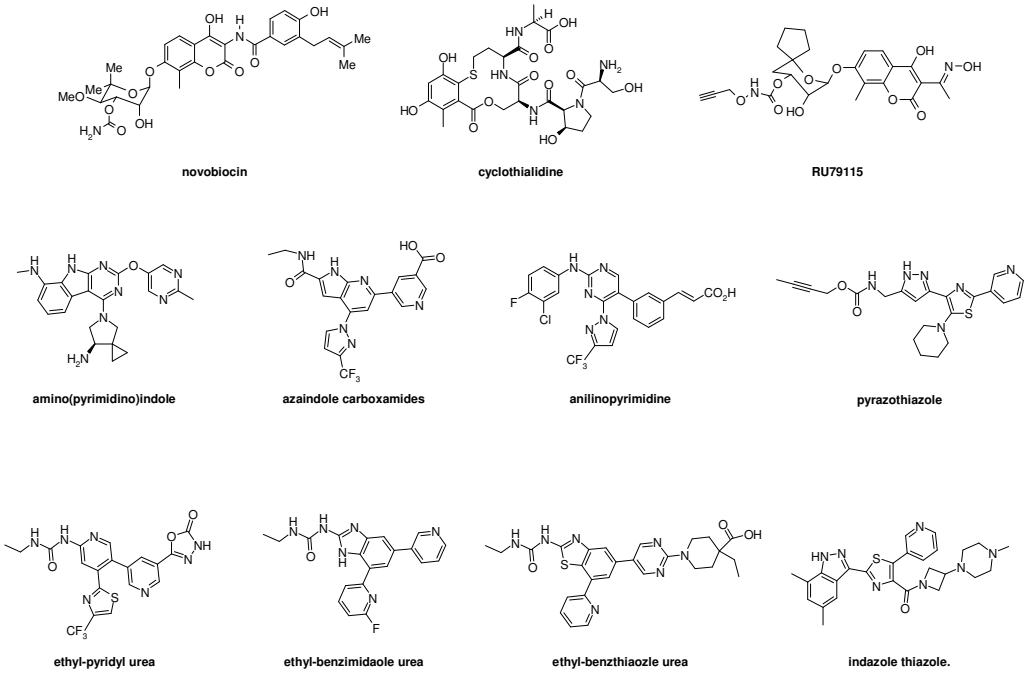

Figure 2. A sampling of ATP-competitive bacterial topoisomerase inhibitors.

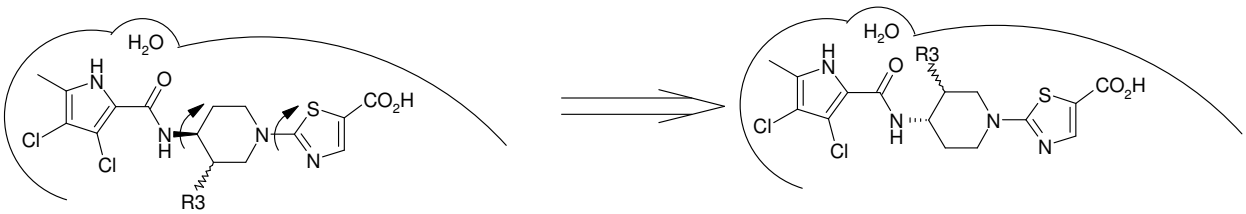

Figure 3. 4*S*-carboxamides **24** and **26** would be accommodated by a 180° rotation of the piperidine ring.

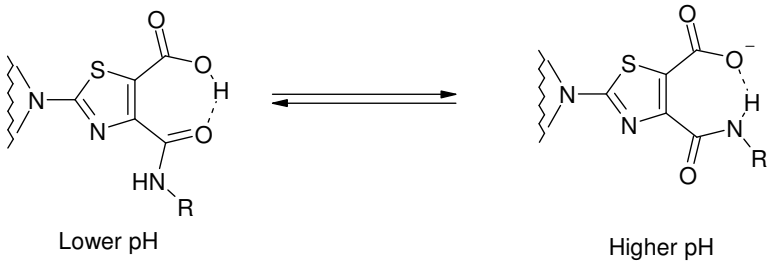

Figure 4. Intramolecular H-bonds to thiazole amide substituents

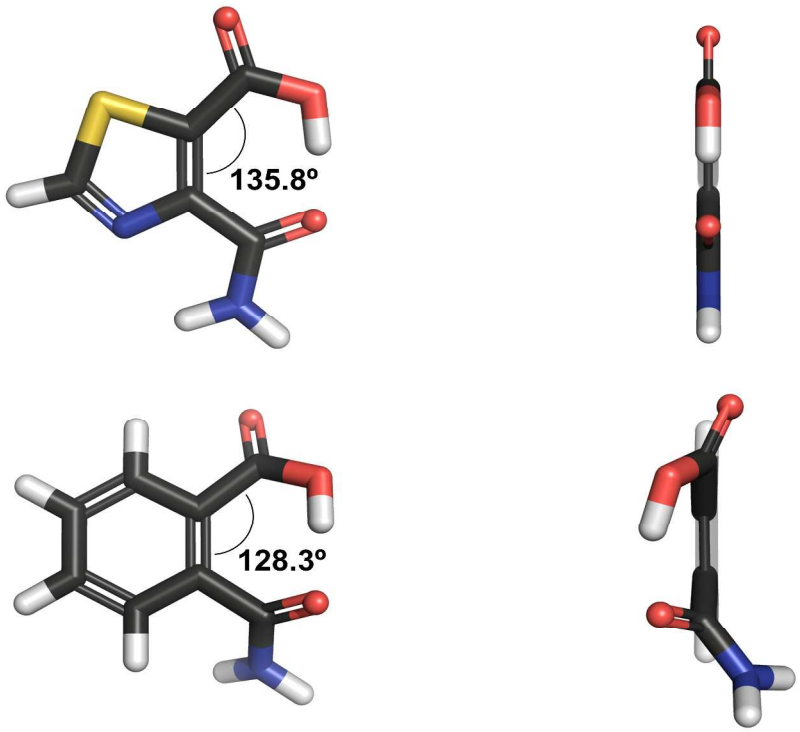

Figure 5. Face and edge views of optimized geometrics for vicinal thiazole carboxylic acid-carboxamide (top) and phthalamic acid (bottom). Geometries were optimized at the B3LYP/6-311++g** level of theory.

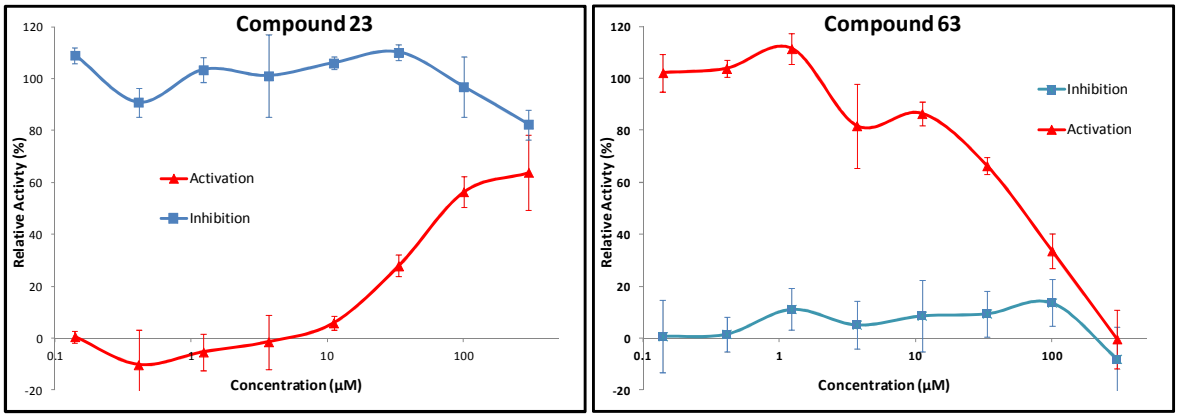

Figure 6 – Inhibition and Activation of human MRP2 ATPase activity for **23** (left) and **63** (right). Error bars represent ± standard error of the mean.

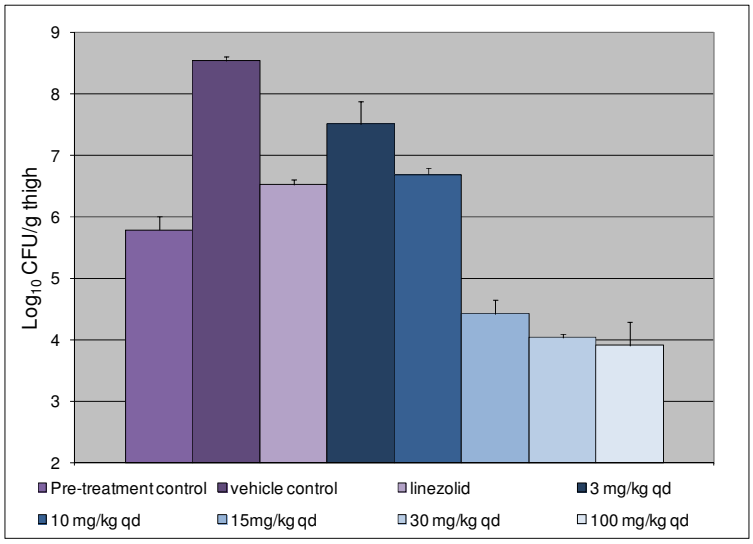

Figure 7. Efficacy of **63** against *S. aureus* ARC516 in a neutropenic mouse thigh infection model. **63** was administered by intraperitoneal injection. Error bars represent ± standard error of the mean.

Scheme 1. General Synthesis of Compounds **1, 2** and **22-90**

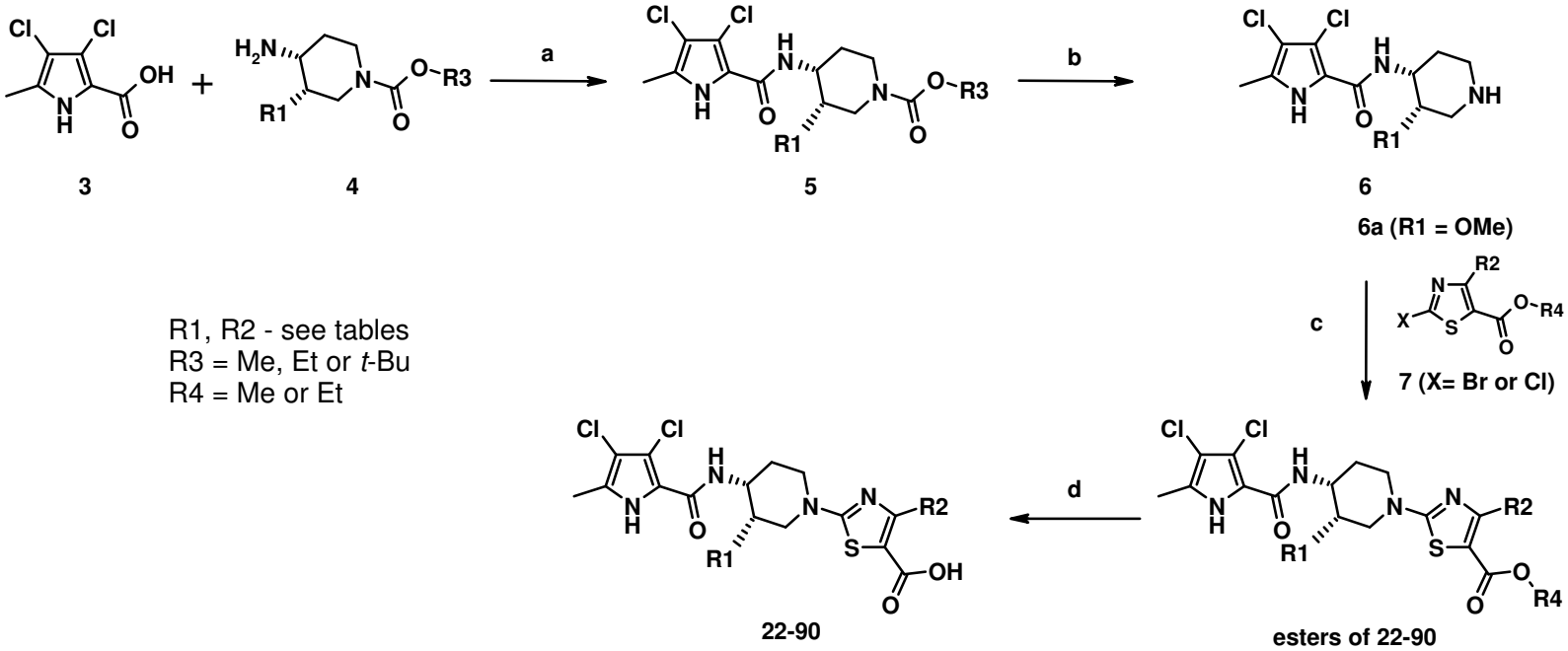

Reagents and conditions: (a) HOBt, NMM, EDC, CH_2Cl_2 (b) NaOH (1N, aq), MeOH or iodotrimethylsilane, CH_2Cl_2 or $Ba(OH)_2$, MeOH, water, 130 ˚C for R3 = Et; HCl-dioxane for R3 = *t*-Bu (c) base, NMP, 80 ˚C (d) 2N LiOH or NaOH, MeOH, water, 100 ˚C or $Ba(OH)_2$, MeOH, water, 80 ˚C

Scheme 2. Synthesis of 3-methoxy-4-aminopipeperidine intermediates (Compounds **4**, where R1= OMe, R3 = Et both racemic and chiral)

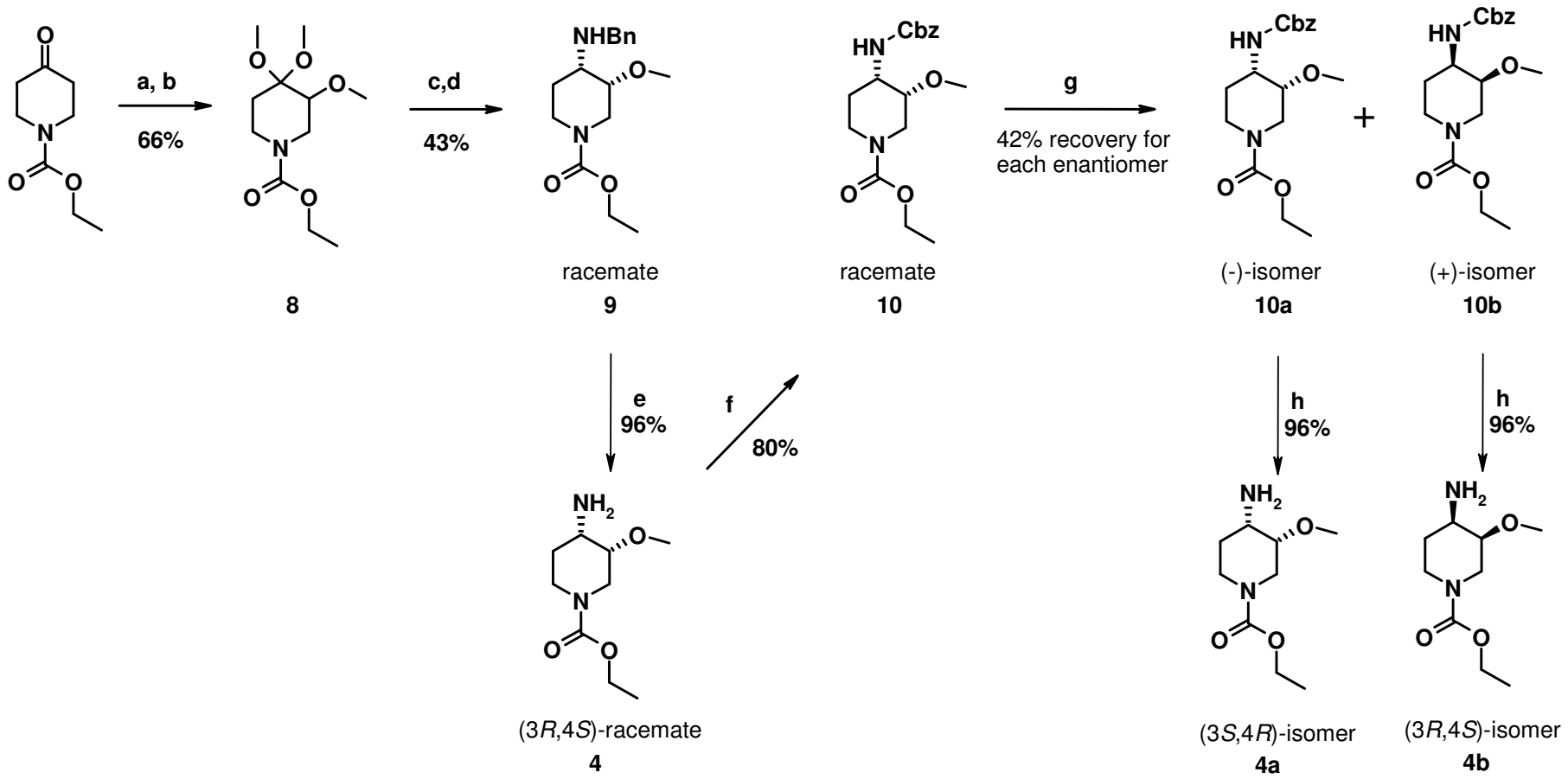

Reagents and conditions: (a) $PhI(OAc)_2$, KOH, MeOH (b) NaH, CH_3I, THF (c) 5% H_2SO_4, THF (d) benzylamine, $NaBH(OAc)_3$ (e) 10% Pd/C, $HCO_2^-NH_4^+$ (f) CbzCl, $NaHCO_3$ (g) chiral chromatography – Chiralcel OJ column (h) H_2, HCl, Pd/C

Scheme 3. Synthesis of 3-position ketal piperidine Compounds **39**, **42-46**

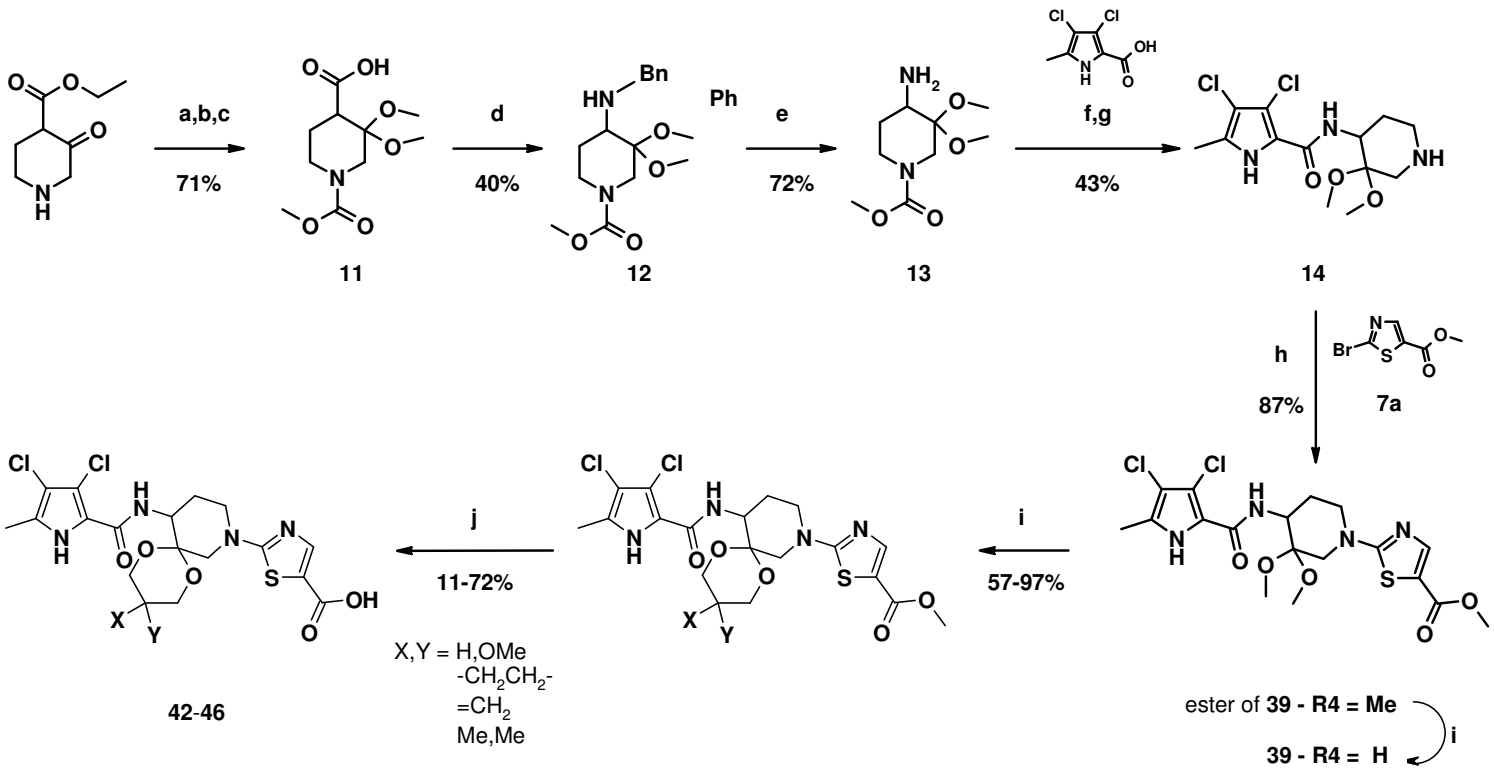

Reagents and conditions: (a) K_2CO_3, methyl chloroformate, water, 0 ˚C (b) trimethylorthoformate, *p*-TsOH, MeOH, reflux (c) $Ba(OH)_2$, MeOH, water (d) ethyl chloroformate, Et_3N, NaN_3, water, 0 ˚C; benzyl alcohol, toluene reflux (e) 10% Pd/C, H_2, EtOH, rt (f) HOBt, NMM, EDC, CH_2Cl_2, rt (g) $Ba(OH)_2$, MeOH, water, 130 °C (h) DIEA, NMP, 80 ˚C; (i) propanediols, *p*-TsOH, toluene, reflux (j) 2N LiOH, MeOH, water, 100 ˚C

Scheme 4. Synthesis of common intermediate thiazole acid-ester intermediates for Compounds **51**-**53**, **61**-**72**

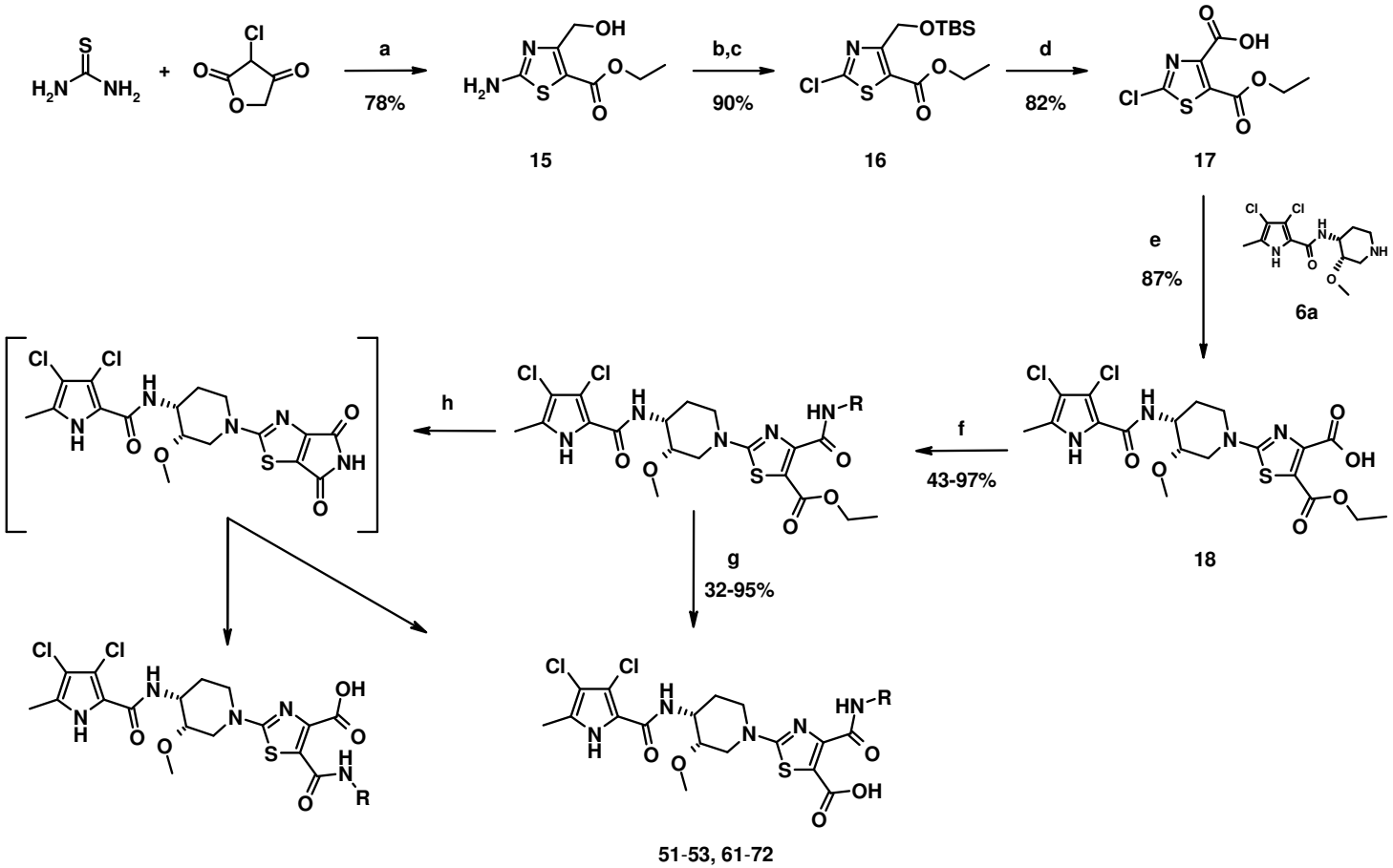

Reagents and conditions: (a) EtOH, reflux (b) TBDMS-Cl, imidazole, CH_2Cl_2, rt (c) $CuCl_2$, *tert*-butyl nitrite, CH_3CN, rt (d) CrO_3, H_2SO_4, acetone, 0 ˚C (e) DIEA, NMP or DMF, 80 ˚C (f) amine, HATU, triethylamine, DMF, rt (g) $Ba(OH)_2$, MeOH, water, rt (h) LiOH or NaOH, MeOH, water, rt

Scheme 5. General synthesis of heterocyclic substituted thiazoles and Compounds **73-90**

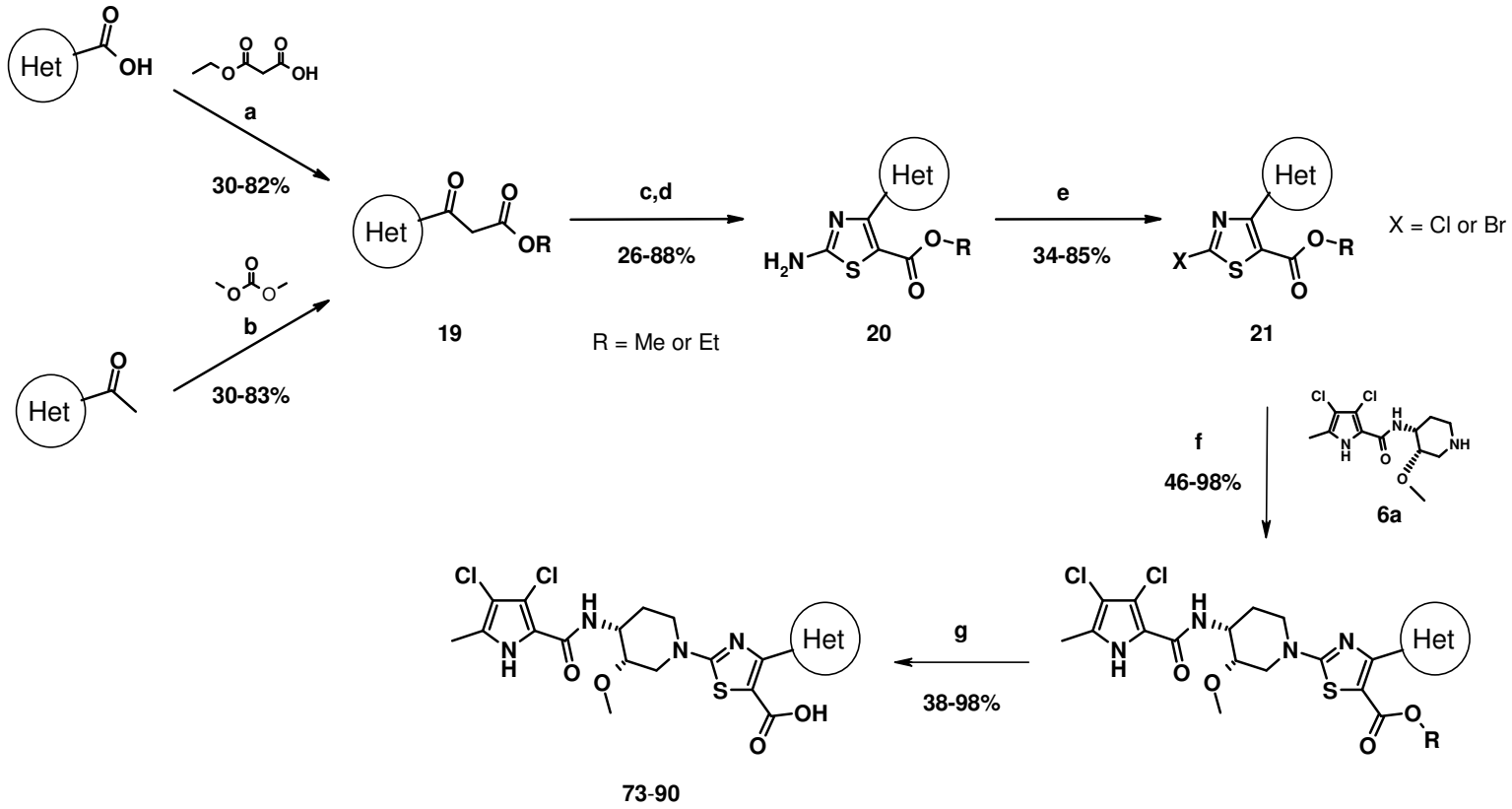

Reagents and conditions: (a) CDI, MeMgBr (1N in THF), THF, 0 ˚C (b) NaH, 0 ˚C (c) NIS, Amberlyst-15 resin, EtOAc, rt (d) thiourea, MeOH, reflux (e) $NaNO_2$, HCl or *t*-Bu-O-N=O, $CuBr_2$, CH_3CN, 0 ˚C (f) DIEA, NMP or DMF, 80-100 ˚C (g) LiOH or NaOH, MeOH, water, rt

Table 1. Influence of Piperidine Configuration on Topoisomerase Inhibitory Potency and MIC Values

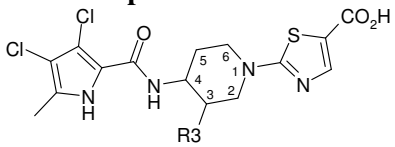

Cmpd	Config. @ 3,4-position	R3	Sau GyrB IC_{50} (nM)	Eco ParE IC_{50} (nM)	MICs (µg/mL)							
					Spn[a]	Spy[b]	MSSA[c]	MRQR[d] Sau	Hin[e]	Mca[f]	Eco[g]	Eco[g] *tolC*⁻
1	NA**	H	62	7800	0.81	0.79	11	13	0.5	2.2	>64	0.22
2	(*S*,*R*)-	F	<10	160	0.078	0.092	1.3	2.2	0.30	0.046	>64	0.081
22	*rel*-(*S*,*R*)-	OMe	<10	910	0.063	ND*	1	1	0.30	0.076	>64	0.35
23	(*S*,*R*)-	OMe	<10	240	0.016	ND	0.32	0.5	0.18	0.031	64	0.18
24	(*S*,*S*)-	OMe	6400	ND	>64	ND	>64	>64	>64	64	>64	64
25	(*R*,*R*)-	OMe	110	ND	8	ND	>64	>64	16	2	>64	2
26	(*R*,*S*)-	OMe	140	ND	1	ND	32	32	16	2	>64	8

[a]Spn: *S. pneumonia*; [b]Spy: *S. pyogenes* [c]Methicillin sensitive *S. aureus*; [d]Methicillin resistant, quinolone resistant *S. aureus*; [e]*H. influenzae*; [f]*M. catarrhalis*; [g]*E. coli*; *ND = not determined; **NA = not applicable

Table 2. Variation of Piperidine Substitution

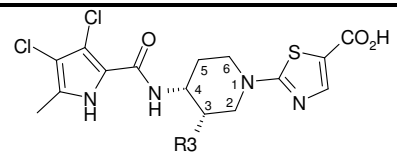

Cmpd	Configuration	R3	LogD	PPB (% f_u)	Solubility (µM)	IC_{50} (nM) Sau GyrB	IC_{50} (nM) Eco ParE	MICs (µg/mL) Spn[a]	Spy[b]	MSSA[c]	MRQR[d] Sau	Hin[e]	Mca[f]	Eco[g]	Eco[g] *tolC*⁻
23	chiral	OCH_3	ND*	7.1	ND	<10	240	0.016	ND	0.32	0.5	0.18	0.031	64	0.18
27	racemic	OH	-0.67	ND	ND	16	1800	0.5	ND	16	16	1.0	4	>64	1
28	racemic	OC_2H_5	0.67	3.1	ND	<10	190	0.031	ND	1	2	2	0.13	>8	1
29	racemic	$OCH_2C{=}CH_2$	ND	ND	ND	<10	150	<0.063	<0.063	0.5	1	0.5	<0.063	>8	0.13
30	chiral	$OCH_2C{\equiv}CH$	0.44	3.0	>1000	<10	24	0.016	0.016	0.25	0.25	0.13	0.016	>8	0.13
31	racemic	$OCH_2CH_2OCH_3$	0.06	9.4	ND	<10	190	0.5	ND	>8	>8	8	1	>8	2
32	racemic	CH_3	0.54	2.3	ND	14	1100	0.5	ND	4	4	2	0.5	>8	0.5
33	racemic	CH_2OCH_3	0.06	5.2	ND	54	ND	4	ND	>8	>8	>8	2	>8	1
34	racemic	CH_2OH	-0.42	ND	ND	18	ND	8	ND	>64	>64	16	1	>64	1
35	racemic	Cl	0.75	0.8	ND	<10	59	0.044	ND	0.35	2	0.18	0.11	>8	0.35
36	racemic	SCH_3	0.72	1.5	>1000	<10	47	0.016	0.016	0.13	0.25	0.13	<0.008	>8	0.25
37	racemic	SO_2CH_3	-1.1	13	>1000	<10	49	>8	>8	>8	>8	>8	>8	>8	>8
38	racemic	N_3	0.53	3.8	>1000	<10	97	<0.063	<0.063	0.13	0.25	<0.063	<0.063	32	<0.063

[a]Spn: *S. pneumonia*; [b]Spy: *S. pyogenes* [c]Methicillin sensitive *S. aureus*; [d]Methicillin resistant, quinolone resistant *S. aureus*; [e]*H. influenzae*; [f]*M. catarrhalis*; [g]*E. coli*; *ND = not determined

Table 3. Influence of Piperidine Ketals

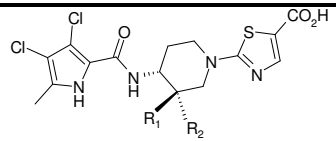

Cmpd	R_1,R_2	LogD	PPB (% f_u)	Solu-bility (µM)	Sau GyrB IC_{50} (nM)	Eco ParE IC_{50} (nM)	MICs (µg/mL)							
							Spn[a]	Spy[b]	MSSA[c]	MRQR[d] Sau	Hin[e]	Mca[f]	Eco[g]	Eco[g] *tolC*[-]
22	H,OCH_3	0.23	ND*	940	<10	910	0.063	ND*	1	1	0.30	0.076	>64	0.35
39	-OCH_3,-OCH_3	0.24	1.8	>1000	14	700	0.13	0.25	2	2	1	0.5	>64	0.5
40	-OCH_2CH_2O-	-0.39	7.5	>1000	18	1800	2	2	32	64	32	1	>64	1
41	-$OCH_2CH_2CH_2O$-	0.40	3.0	>1000	<10	200	0.063	0.13	2	4	1	0.13	>64	1
42	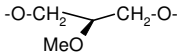	0.15	5.3	>1000	<10	250	0.063	0.5	4	8	2	1	>64	1
43	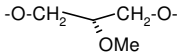	-0.18	5.3	>1000	<10	51	0.063	0.25	4	4	1	0.13	>64	1
44		1.07	2	>1000	<10	130	<0.063	<0.063	0.5	0.5	0.25	<0.063	>64	1
45		0.88	1.2	>1000	<10	41	<0.063	<0.063	0.5	0.5	0.13	<0.063	>64	1
46	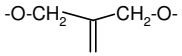	0.82	0.60	>1000	<10	170	<0.063	<0.063	1	2	2	<0.063	>64	0.5

[a]Spn: *S. pneumonia*; [b]Spy: *S. pyogenes* [c]Methicillin sensitive *S. aureus*; [d]Methicillin resistant, quinolone resistant *S. aureus*; [e]*H. influenzae*; [f]*M. catarrhalis*; [g]*E. col;* *ND = not determined

Table 4. Variation of Piperidine Aromatic Groups

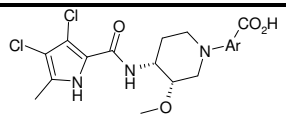

Cmpd	Ar	LogD	PPB (% f_u)	Solubility (µM)	Sau GyrB IC_{50} (nM)	Eco ParE IC_{50} (nM)	MICs (µg/mL) Spn[a]	Spy[b]	MSSA[c]	MRQR[d]	MRQR[d] MIC/f_u	Hin[e]	Mca[f]	Eco[g]	Eco[g] *tolC*⁻	Rat Cl (mL/min/kg)
23	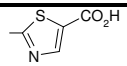	ND*	7.1	ND	<10	240	0.016	ND	0.32	0.5	7	0.18	0.031	64	0.18	52
47		1.2	1.8	450	<10	65	0.013	<0.008	0.031	0.053	2.9	0.072	0.008	>8	0.25	26
48	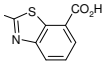	1.7	<1	<1	<10	14	0.032	ND	0.031	0.031	>31	0.031	<0.001	8	0.25	60
49	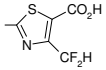	0.52	ND	690	<10	ND	0.063	0.13	2	2	-	1	0.063	>8	0.5	70
50		0.36	1.9	890	<10	ND	0.020	0.020	0.063	0.063	3.7	0.15	0.020	30	0.26	9.3
51		1.3	2.0	56	<10	72	0.016	0.013	0.063	0.063	3.15	0.14	0.011	18	0.30	14
52	(±) 	-1.0	13	>1000	<10	420	4	ND	8	>8	>62	8	2	>8	2	ND
53	(±) 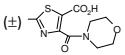	-0.99	14	200	<10	ND	2	ND	8	>8	>57	8	2	>8	4	ND
54	(±) 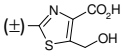	-0.27	2.9	ND	<10	ND	2	ND	>8	>8	17	8	1	>8	1	ND
55		0.44	3.4	>1000	<10	160	0.125	ND	0.5	1	29	0.35	0.063	>8	0.5	ND
56	(±) 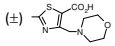	1.4	5.7	>1000	<10	ND	0.25	0.25	2	2	35	4	1	0.13	>8	0.25
57	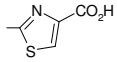	0.25	2.2	930	<10	ND	0.020	0.035	0.20	0.32	15	0.10	0.050	>8	0.10	49
58	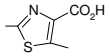	1.2	0.7	>1000	<10	370	0.031	0.063	0.13	0.13	19	0.25	0.063	>8	0.25	ND
59	(±) 	-0.63	0.5	ND	<10	ND	1	ND	>8	ND	160	>8	2	>8	1	ND
60	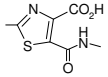	ND	<1	>1000	ND	ND	>32	ND	ND	2	>200	ND	ND	>64	2	ND

[a]Spn: *S. pneumonia*; [b]Spy: *S. pyogenes* [c]Methicillin sensitive *S. aureus*; [d]Methicillin resistant, quinolone resistant *S. aureus*; [e]*H. influenzae*; [f]*M. catarrhalis*; [g]*E. coli*; *ND = not determined

Table 5. Variation of Thiazole Carboxamides

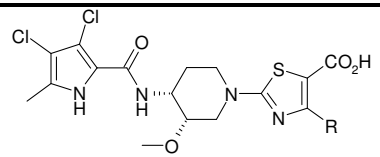

Cmpd	R	LogD	PPB (% f_u)	Solubility (µM)	Sau GyrB IC_{50} (nM)	Eco ParE IC_{50} (nM)	MICs (µg/mL) Spn[a]	Spy[b]	MSSA[c] Sau	MRQR[d] Sau	MRQR[d] MIC/f_u	Hin[e]	Mca[f]	Eco[g]	Eco[g] *tolC*⁻	Rat Cl (mL/min/kg)
51		1.3	2.0	56	<10	72	0.016	0.013	0.063	0.063	3.15	0.14	0.011	18	0.30	14
61		0.85	4.3	280	<10	120	0.039	0.039	0.5	0.5	12	0.16	0.020	>8	0.32	NT
62	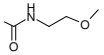	1.2	2.7	880	<10	53	0.018	0.017	0.078	0.089	3.3	0.15	0.017	24	0.62	9.5
63	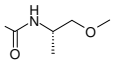	1.4	2.5	960	<10	73	0.016	0.014	0.036	0.057	2.3	0.13	<0.008	24	0.94	14
64	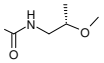	ND*	2.7	ND	<10	43	0.016	<0.008	0.031	0.031	1.1	0.13	<0.008	>8	0.5	13
65	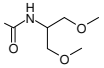	1.0	2.1	860	<10	51	0.016	0.016	0.050	0.049	2.3	0.10	<0.008	23	1.3	18
66	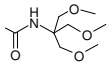	1.9	4.7	720	<10	42	0.016	0.016	0.031	0.031	0.66	0.15	0.008	29	1.3	18
67	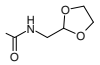	0.76	2.8	940	<10	36	0.040	0.020	0.063	0.10	3.6	0.10	0.013	>8	0.79	33
68		1.2	3.6	>1000	<10	100	0.016	0.016	<0.06	<0.06	<1.8	0.16	0.008	14	0.76	38
69		1.0	3.2	620	<10	180	0.016	0.016	0.063	0.084	2.6	0.11	0.016	11	0.5	34
70	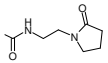	ND	7.6	870	<10	53	<0.06	<0.06	0.35	1.4	18	0.5	<0.063	64	0.71	NT
71	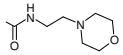	1.0	5.4	>1000	<10	59	0.031	0.031	0.25	0.5	9.2	0.25	0.031	>8	0.25	NT
72		-0.15	7.1	>1000	<10	110	0.25	0.25	2.0	4.0	56	1.4	0.35	>64	1	NT

[a]Spn: *S. pneumonia*; [b]Spy: *S. pyogenes* [c]Methicillin sensitive *S. aureus*; [d]Methicillin resistant, quinolone resistant *S. aureus*; [e]*H. influenzae*; [f]*M. catarrhalis*; [g]*E. coli;* *ND = not determined

Table 6. Variation of Thiazole Heterocycles

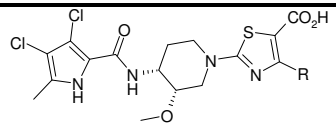

Cmpd	R	LogD	PPB (% f_u)	Solubility (µM)	Sau GyrB IC_{50} (nM)	Eco ParE IC_{50} (nM)	MICs (µg/mL) *Spn*[a]	*Spy*[b]	MSSA[c] *Sau*	MRQR[d] *Sau*	MRQR[d] MIC/f_u	*Hin*[e]	*Mca*[f]	*Eco*[g]	*Eco*[g] tolC[-]	Rat Cl (mL/min/kg)
73		1.2	3.9	540	<10	54	0.007	0.010	0.031	0.018	0.46	0.13	0.008	>8	0.5	2.7
74		0.15	3.2	630	<10	85	0.007	0.016	0.063	0.040	1.25	0.12	0.026	32	0.46	17
75		0.54	9.6	350	<10	68	0.008	0.016	0.090	0.12	1.25	0.20	0.031	23	0.5	34
76		1.7	4.2	350	<10	43	<0.06	<0.06	<0.06	0.031	0.74	0.12	<0.06	16	0.5	3.8
77		0.35	1.1	260	<10	120	<0.10	0.40	3.2	3.2	290	1.6	0.40	>100	0.80	ND
78		1.7	3.6	ND*	<10	68	0.016	0.016	0.025	0.050	1.4	0.25	0.016	32	1	6.3
79		0.24	7.1	170	<10	0.70	<0.06	<0.06	<0.06	<0.06	<0.9	0.50	<0.06	16	0.25	27
80		ND	3.6	ND	<10	71	<0.06	<0.06	<0.06	<0.06	1.75	0.25	<0.06	16	ND	6.3
81		>3	1.1	12	<10	120	<0.06	<0.06	<0.06	<0.06	5.2	0.25	<0.06	8	<0.06	ND
82		2.5	1.9	3	<10	62	<0.06	<0.06	0.13	0.13	6.8	2	<0.06	16	<0.06	ND
83		1.7	ND	740	<10	87	<0.06	<0.06	0.5	0.17	-	0.5	<0.06	64	0.18	ND
84		>2.5	<1	<1	<10	0.12	<0.06	0.080	0.63	1	100	1	<0.06	>64	<0.06	ND
85		0.07	1.5	630	<10	79	<0.06	<0.06	0.13	0.13	8.7	0.13	<0.06	32	0.5	110
86		0.80	3.7	770	<10	ND	0.011	0.031	0.13	0.19	5.1	0.23	ND	60	0.23	9.6
87		2.0	2.7	36	1.2	35	0.011	0.031	0.25	0.58	21	1.0	ND	46	0.51	ND
88		>2.5	0.3	<1	<9.8	40	<0.06	<0.06	<0.06	<0.06	<21	0.5	<0.06	8	0.13	ND
89		3.6	<1	16	<9.8	45	<0.06	<0.06	<0.06	<0.06	<6.3	0.13	<0.06	8	0.13	ND
90		3.0	<1	<1	<9.8	51	<0.06	<0.06	<0.06	<0.06	<6.3	0.5	<0.06	4	<0.06	ND

[a]Spn: *S. pneumonia*; [b]Spy: *S. pyogenes;* [c]Methicillin sensitive *S. aureus*; [d]Methicillin resistant, quinolone resistant *S. aureus*; [e]*H. influenzae*; [f]*M. catarrhalis*; [g]*E. coli;* *ND = not determined

Table 7. PK properties of selected compounds

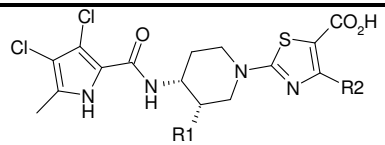

Cmpd	R1	R2	pK_a	Mouse ppb (% f_u)	Mouse F (%)	Mouse Cl (mL/min/kg)	Rat ppb (% f_u)	Rat F (%)	Rat Cl (mL/min/kg)	Dog ppb (% f_u)	Dog F (%)	Dog Cl (mL/min/kg)
1	F	H	3.4	8.9	ND*	15.5	8.6	6.7	54	12	ND	3
23	OMe	H	3.6	ND	ND	99	ND	6.7	66	22	ND	26
62	OMe	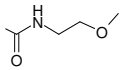	4.4	5.85	57	57	3.8	34	9.5	8.2	100	3.0
63*	OMe	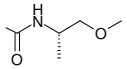	4.2	4.7	100	10	3.4	81	17	6.2	96	0.64
65	OMe	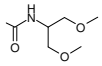	4.5	4.2	25	5.35	3.8	ND	18	12	29	1.6
73	OMe		5.4	7.4	ND	ND	7.15	ND	2.5	13	18	0.73
74	OMe		4.5	9.7	74	7.4	8.8	65	16	20	70	1.6
75	OMe		5.2	18	100	22	19	100	31	24	100	1.9

*ND = not determined

Table 8 – Clearance of selected compounds in Wistar and TR$^-$ rats

Compound	Wistar Cl (mL/min/kg)	TR$^-$ Cl (mL/min/kg)
1	78 ± 53	20 ± 7.4
23	34 ± 30	9.1 ± 3.9
62	2.1 ± 0.2	1.5 ± 0.1
63	4.0 ± 2.4	2.1 ± 0.6
65	13 ± 6.6	3.0 ± 0.9
75	18 ± 2	9.3 ± 0.5

Table 9 – Influence of select compounds on transporter ATPase activity

	Human MRP2		Rat Mrp2	
Compound	EC_{50} of Stimulation (μM)	IC_{50} of Inhibition (μM)	EC_{50} of Stimulation (μM)	IC_{50} of Inhibition (μM)
1	145	>200	27	>200
23	71	>200	38	>200
62	>200	100	>200	78
63	>200	59	>200	200
65	>200	200	>200	75
74	140	>200	110	>200

Table 10 – Efficacy of pyrrolamides against *S. aureus* ARC516 in the neutropenic thigh infection model

Compound	total daily dose/regimen	mean AUC µg.h/mL	mean free AUC µg.h/mL	mean delta log CFU*	MIC µg/mL
63	30 mg/kg q24	116	5.45	1.51	0.03
65	30 mg/kg q24	148	6.26	-0.16	0.03
74	30 mg/kg q24	204	19.8	1.54	0.03
75	30 mg/kg q6	37.6	6.7	-1.57	0.06

* relative to the pre-treatment inoculum

Table 11 – MIC_{90}s of 63 and Comparators

		63	Levo-floxacin	Azithro-mycin
Pathogen	# of strains	MIC_{90}s (µg/mL)		
S. aureus	**200**	**0.06**	**32**	**>128**
Methicillin Resistant	110	0.06	64	>128
E. faecalis	**100**	**0.015**	**32**	**>128**
Vancomycin Resistant	8*	0.015	64	>128
E. faecium	**100**	**0.06**	**>128**	**>128**
Vancomycin Resistant	50	0.06	>128	>128
H. influenzae	**200**	**0.25**	**0.015**	**2**
Amoxicillin Resistant	40	0.25	0.015	2

*Highest MIC for the number of indicated strains

Table 12 Characterization of *Staphylococcus aureus* variants

Strain	**Selection[a]**	**MIC (µg/mL)**		**Ratio**		**Sequence changes**	
		Linezolid	**63**	**Linezolid**	**63**	**GyrB**	**ParE**
ARC516	-	1	0.016	1	1	-	-
ARC516-1F	2X	1	0.25	1	16	T173A	None
ARC516-2F	2X	0.5	0.25	0.5	16	T173A	None
ARC1692	-	2	0.06	1	1	-	-
ARC1692-1F	2X	2	0.5	1	8	R144I	None
ARC1692-2F	2X	2	0.5	1	8	R144I	None
ARC2381	-	2	0.016	1	1	-	-
ARC2381-2F	2X	2	0.13	1	8	T173A	None
ARC2381-3F	2X	2	0.13	1	8	T173A	None
ARC2398	-	2	0.03	1	1	-	-
ARC2398-1F	2X	2	0.5	1	16	R144I	None
ARC2398-2F	2X	2	0.5	1	16	R144I	None

[a]Fold increase of drug concentration over the concentration that prevented confluent bacterial growth.

Table of Contents graphic